THE EUROPEAN
PHYSICAL JOURNAL C

Search for rare decays of Z and Higgs bosons to J/ψ and a photon in proton-proton collisions at $\sqrt{s} = 13$ TeV

CMS Collaboration[*]

CERN, 1211 Geneva 23, Switzerland

Abstract A search is presented for decays of Z and Higgs bosons to a J/ψ meson and a photon, with the subsequent decay of the J/ψ to $\mu^+\mu^-$. The analysis uses data from proton-proton collisions with an integrated luminosity of 35.9 fb^{-1} at $\sqrt{s} = 13$ TeV collected with the CMS detector at the LHC. The observed limit on the Z → J/ψγ decay branching fraction, assuming that the J/ψ meson is produced unpolarized, is 1.4×10^{-6} at 95% confidence level, which corresponds to a rate higher than expected in the standard model by a factor of 15. For extreme-polarization scenarios, the observed limit changes from −13.6 to +8.6% with respect to the unpolarized scenario. The observed upper limit on the branching fraction for H → J/ψγ where the J/ψ meson is assumed to be transversely polarized is 7.6×10^{-4}, a factor of 260 larger than the standard model prediction. The results for the Higgs boson are combined with previous data from proton-proton collisions at $\sqrt{s} = 8$ TeV to produce an observed upper limit on the branching fraction for H → J/ψγ that is a factor of 220 larger than the standard model value.

1 Introduction

A new boson with a mass of 125 GeV was observed in data from the ATLAS and CMS experiments at the CERN LHC [1–7]. All measurements of the properties of this boson are consistent with those of the Higgs boson (H) of the standard model (SM). However, the Yukawa couplings of the Higgs boson to the first- and second-generation quarks are currently only weakly constrained. Rare exclusive decays of the Higgs boson to mesons in association with a photon can be used to explore such couplings. For example, the H → J/ψγ decay can probe the Higgs boson coupling to the charm quark [8]. The corresponding decay, Z → J/ψγ, can be used as an experimental benchmark in the search for H → J/ψγ [9,10], and in checking approaches to factorization in quantum chromodynamics (QCD) used to estimate

branching fractions ($\mathcal{B}$) in radiative decays of electroweak bosons [11].

Both Z and Higgs boson decays receive contributions from direct and indirect processes. In the direct process, Z and Higgs bosons couple to charm quarks, and charm quarks then hadronize to form J/ψ mesons. In the indirect process, the Z and Higgs bosons decay through quark or W boson loops to $\gamma\gamma^*$, and the γ^* then converts to a $c\bar{c}$ resonant state. The lowest order Feynman diagrams for these decay modes are shown in Fig. 1. The latest SM calculations of the branching fractions of both decays, taking into account the interference between direct and indirect processes, are [12,13]:

$$\mathcal{B}_{SM}(Z \rightarrow J/\psi\gamma) = (9.0^{+1.5}_{-1.4}) \times 10^{-8}, \tag{1}$$

$$\mathcal{B}_{SM}(H \rightarrow J/\psi\gamma) = (3.0^{+0.2}_{-0.2}) \times 10^{-6}. \tag{2}$$

Modified Hc$\bar{c}$ couplings can arise in certain extensions of the SM [14]. For example, within the context of effective field theory, the Hc$\bar{c}$ coupling may be modified in the presence of a dimension-six operator, leading to an enhancement of coupling relative to the SM at the cutoff scale Λ that can be as small as 30 TeV. This provides no other signature of new physics at the LHC. In the two Higgs doublet model with minimal flavor violation [15,16], the Hc$\bar{c}$ coupling can be significantly enhanced by breaking flavor symmetry, while other couplings are not severely affected. The composite pseudo-Nambu-Goldstone boson model [17] parametrizes the coupling by the degree of compositeness and compositeness scale. The coupling can be constrained through a direct experimental search for the composite particles associated with the charm quark [18].

Deviations from SM predictions for the couplings can affect the interference terms and result in changes to the branching fractions. For example, the shift in the branching fraction for H → J/ψγ can be more than 100% if the Hc$\bar{c}$ coupling deviates from its SM value by more than a factor of 2 [8]. Since this Higgs boson decay is sensitive to the Hc$\bar{c}$ coupling, a measurement of the branching fraction can verify whether the Higgs boson couples to second-generation quarks with the strength predicted by the SM.

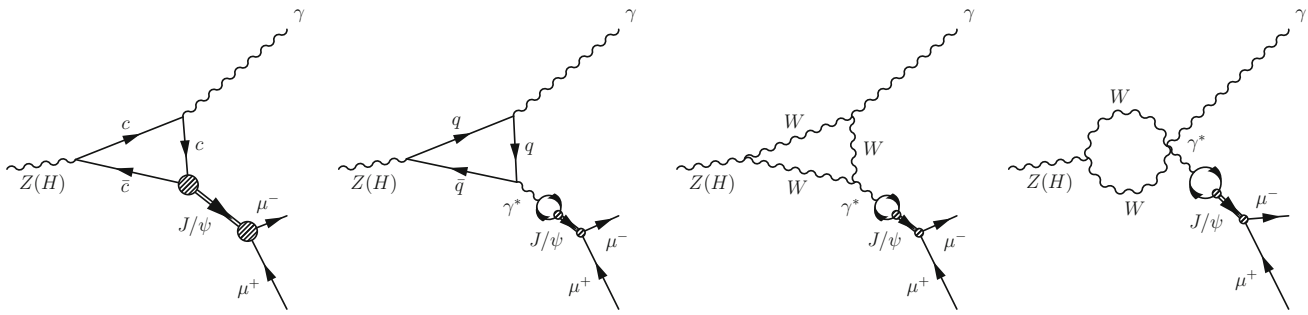[*] e-mail: cms-publication-committee-chair@cern.ch

Springer

Fig. 1 Lowest order Feynman diagrams for the Z (or H)$\rightarrow$ J/$\psi\gamma$ decay. The left-most diagram shows the direct and the remaining diagrams the indirect processes

The ATLAS experiment has searched for the decay Z $\rightarrow$ J/$\psi\gamma$ in proton-proton (pp) collisions collected at $\sqrt{s} =$ 8 TeV [19]. The respective observed and expected upper limits at 95% confidence level (CL) on the branching fraction were reported to be 2.6 and $2.0^{+1.0}_{-0.6} \times 10^{-6}$, where the subscript and superscript reflect the range in the 68% central-quantiles of upper limits assuming a background-only hypothesis. Searches for the H $\rightarrow$ J/$\psi\gamma$ decay were performed by ATLAS and CMS in pp collisions collected at $\sqrt{s} =$ 8 TeV [19,20]. The respective observed and expected upper limits in the branching fractions were 1.5 and $1.2^{+0.6}_{-0.3} \times 10^{-3}$ from ATLAS, and 1.5 and $1.6^{+0.8}_{-0.8} \times 10^{-3}$ from CMS. The ATLAS experiment performed similar searches for both the Z and Higgs boson decays in pp collisions collected at $\sqrt{s} =$ 13 TeV. The respective observed and expected upper limits on the branching fractions were 2.3 and $1.1^{+0.5}_{-0.3} \times 10^{-6}$ for the Z boson decay, and 3.5 and $3.0^{+1.4}_{-0.8} \times 10^{-4}$ for the Higgs boson decay [21]. The ATLAS experiment also searched for the H $\rightarrow$ c$\bar{c}$ decay in pp $\rightarrow$ ZH production in data collected at $\sqrt{s} =$ 13 TeV [22], and reported observed and expected limits on the ratio σ(pp $\rightarrow$ ZH) $\times \mathcal{B}$(H $\rightarrow$ c$\bar{c}$) relative to the SM prediction of 110 and 150^{+80}_{-40} respectively, where σ(pp $\rightarrow$ ZH) $\times \mathcal{B}$(H $\rightarrow$ c$\bar{c}$) is the upper limit for the cross section.

The results presented in this paper are based on pp collisions at $\sqrt{s} =$ 13 TeV recorded with the CMS detector, corresponding to an integrated luminosity of 35.9 fb^{-1}.

2 The CMS detector

A detailed description of the CMS detector, together with a definition of the coordinate system used and the relevant kinematic variables, can be found in Ref. [23]. The central feature of the CMS apparatus is a superconducting solenoid, 13 m in length and 6 m in internal diameter, providing an axial magnetic field of 3.8 T. Within the solenoid volume are a silicon pixel and strip tracker, a lead tungstate crystal electromagnetic calorimeter (ECAL), and a brass and scintillator

hadron calorimeter (HCAL), each composed of a barrel and two endcap sections. Forward calorimeters extend the pseudorapidity (η) coverage provided by the barrel and endcap detectors. Muons are detected in gas-ionization chambers embedded in the steel flux-return yoke outside the solenoid.

The silicon tracker measures charged particles within the range $|\eta| < 2.5$. It consists of 1440 silicon pixel and 15 148 silicon strip detector modules. For non-isolated particles with transverse momentum, p_T, between 1 and 10 GeV and $|\eta| <$ 1.4, the track resolutions are typically 1.5% in p_T and 25–90 (45–150) μm in the transverse (longitudinal) direction [24].

The ECAL consists of 75 848 crystals, which provide coverage in $|\eta| <$ 1.479 in the barrel region (EB) and 1.479 $< |\eta| <$ 3.000 in the two endcap regions (EE). The preshower detectors, each consisting of two planes of silicon sensors interleaved with a total of $3X_0$ of lead are located in front of the EE [25,26]. In the barrel section of the ECAL, an energy resolution of about 1% is achieved for unconverted or late-converting photons in the tens of GeV energy range. The remaining barrel photons have a resolution of about 1.3% up to $|\eta| = 1$, rising to about 2.5% at $|\eta| = 1.4$. In the endcaps, the resolution of unconverted or late-converting photons is about 2.5%, while the remaining endcap photons have a resolution between 3 and 4% [26].

Muons are measured in the range $|\eta| < 2.4$, with detection planes made using three technologies: drift tubes, cathode strip chambers, and resistive plate chambers. Matching muons to tracks measured in the silicon tracker results in a relative p_T resolution, for muons with p_T up to 100 GeV, of 1% in the barrel and 3% in the endcaps. The p_T resolution in the barrel is better than 7% for muons with p_T up to 1 TeV [27].

A two-tier trigger system selects collision events of interest. The first level (L1) of the CMS trigger system [28], composed of custom hardware processors, uses information from the calorimeters and muon detectors to select the most interesting events in a fixed time interval of less than 4 μs. The high-level trigger processor farm further decreases the event

rate from around 100 kHz to less than 1 kHz, before data storage.

3 Data and simulated samples

The L1 trigger requires the presence of a muon with p_T greater than 5 GeV and an isolated electromagnetic object with p_T greater than 18 GeV. The HLT algorithm requires the presence of a muon and a photon with p_T exceeding 17 and 30 GeV, respectively. No isolation requirement is imposed on the muons because of the small angular separation expected between the muons in signal events. No further isolation constraint is required for the photon. The trigger efficiency for events satisfying the selection used in the analysis is determined using a high-purity ($\sim 97\%$) $Z \to \mu\mu\gamma$ control sample; it is measured to be $82 \pm 0.7\%$ in data and $83 \pm 0.4\%$ in simulated events.

Simulated samples of the Z and Higgs boson decays are used to estimate the expected signal yields and model the kinematic distributions of signal events. The $Z \to J/\psi\gamma \to \mu\mu\gamma$ sample, with $m_Z = 91.2$ GeV [29], is produced with the PYTHIA 8.226 Monte Carlo (MC) event generator [30,31], with hadronization and fragmentation using underlying event tune CUETP8M1 [32]. The parton distribution function (PDF) set used is NNPDF3.0 [33]. The SM Z boson production cross section includes the next-to-next-to-leading order (NNLO) QCD contributions, and the next-to-leading order (NLO) electroweak corrections from FEWZ 3.1 [34] calculated using the NLO PDF set NNPDF3.0. The Z boson p_T is reweighted to match the NLO calculation [35–37].

The $H \to J/\psi\gamma \to \mu\mu\gamma$ sample with $m_H = 125$ GeV is produced with the POWHEG v2.0 MC event generator [35,36] and includes gluon-gluon fusion (ggF), vector boson fusion (VBF), associated vector boson production (VH), and associated top quark pair production (t$\bar{t}$H). The generator is interfaced with PYTHIA 8.212 [30,31] for hadronization and fragmentation with tune CUETP8M1. The PDF set used is NNPDF3.0. The SM Higgs boson cross section is taken from the LHC Higgs cross section working group recommendations [38].

In the SM, the J/ψ meson from the Higgs boson decay must be fully transversely polarized in helicity frame ($\lambda_\theta = +1$, as described in Ref. [39]), because the Higgs boson has spin 0, and the photon is transversely polarized. Since the polarization of the J/ψ meson is not correctly simulated in the signal samples, a reweighting factor is applied to each event to emulate the effect of polarization. The reweighting procedure results in a decrease of the signal acceptance by 7.0%. For the Z boson decay, the helicity of the J/ψ meson depends on that of the Z boson, which can have multiple helicity states. The results from the Z boson polarization measurement [40,41] are not used to constrain the helicity
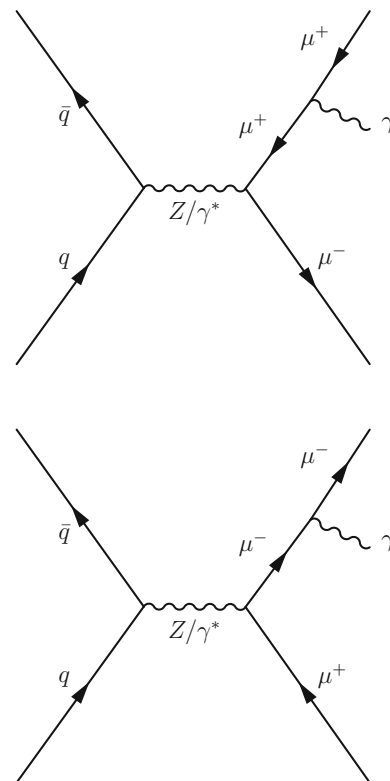

Fig. 2 The lowest order Feynman diagrams for the Drell-Yan process in pp $\to$ Z $\to \mu\mu\gamma$. The background exhibits a peak in $m_{\mu\mu\gamma}$ at the Z boson mass

of the J/ψ meson in this analysis. The nominal results are obtained using a signal acceptance calculated for the unpolarized case. Assuming that the J/ψ is produced with full transverse or longitudinal polarization ($\lambda_\theta = +1$ or -1) changes the acceptance by -7.8% or $+15.6\%$, respectively.

The Drell-Yan process, pp $\to$ Z $\to \mu\mu\gamma$, produces the same final state as the signal. This process exhibits a peak at the Z boson mass, m_Z, in the three-body invariant mass, $m_{\mu\mu\gamma}$, as do the signal events, and it is therefore referred to as a resonant background. This background is included when deriving the upper limit on the branching fraction for $Z \to J/\psi\gamma$. The lowest order Feynman diagrams for the pp $\to$ Z $\to \mu\mu\gamma$ process are shown in Fig. 2. The MADGRAPH5_aMC@NLO 2.6.0 matrix element generator [37] is used to generate a sample of these resonant background events at leading order with the NNPDF3.0 PDF set, interfaced with PYTHIA 8.226 for parton showering and hadronization with tune CUETP8M1. The photons in these events are all produced in final-state radiation from the $Z \to \mu\mu$ decay, and therefore the $m_{\mu\mu\gamma}$ distribution peaks at the Z boson mass without a continuum contribution.

Similarly, the Higgs boson Dalitz decay [42], $H \to \gamma^*\gamma \to \mu\mu\gamma$, is a resonant background to $H \to J/\psi\gamma$ decay. The lowest order Feynman diagrams for the $H \to \gamma^*\gamma$ process are shown in Fig. 3. Samples of the Higgs

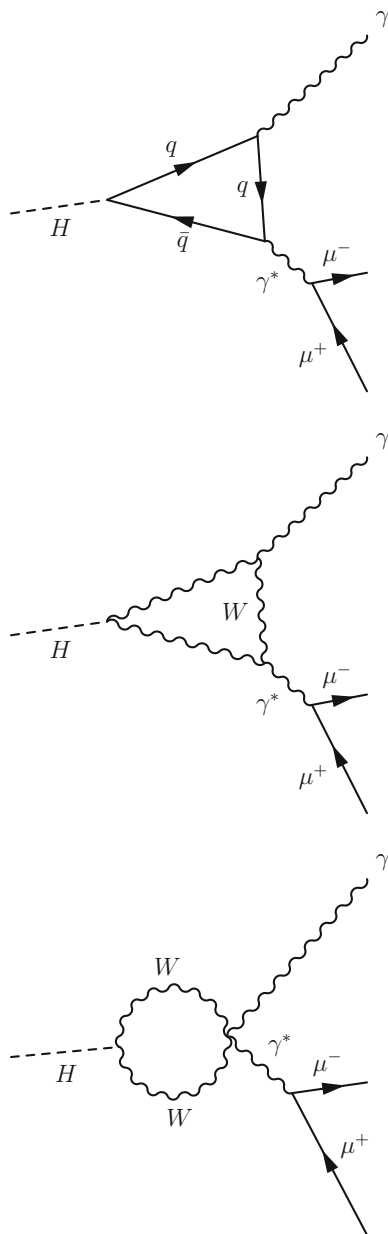**Fig. 3** The lowest order Feynman diagrams for the Higgs boson Dalitz decay of H $\to \gamma^*\gamma \to \mu\mu\gamma$. The background exhibits a peak in $m_{\mu\mu\gamma}$ at the Higgs boson mass

boson Dalitz decays, produced via ggF, VBF, VH modes for $m_H = 125$ GeV, are simulated at NLO using the MAD-GRAPH5_aMC@NLO generator interfaced with PYTHIA 8.212 for parton showering and hadronization. The t$\bar{t}$H contribution is accounted for by scaling the VBF signal to the t$\bar{t}$H production cross section. The branching fraction for H $\to \gamma^*\gamma$ is obtained from the MCFM 7.0.1 program [43]. The other source of resonant background is the decay of a Higgs boson into two muons with a photon radiated from one of the muons. After the event selection, described in Sect. 4, the contribution of this background is negligible.

There are also background processes that do not give resonant peaks in the three-body invariant mass spectrum. These are referred to as nonresonant backgrounds. These processes include: (1) inclusive quarkonium production associated with either jets or photons where energetic jets can be misidentified as a photon (pp $\to$ J/ψ + jets/γ), (2) the Drell-Yan process with associated jets (pp $\to$ Z/γ^*+jets), and (3) associated photons plus jets production (pp $\to \gamma$ + jets). These nonresonant backgrounds, which are discussed in Sect. 5, are modeled using fits to the $m_{\mu\mu\gamma}$ distributions in data.

All generated events are processed through a detailed simulation of the CMS detector based on GEANT4 [44]. Simultaneous pp interactions that overlap the event of interest (pileup) are included in the simulated samples. The distribution of the number of additional pileup interactions per event in the simulation corresponds to that observed in the 13 TeV data collected in 2016.

4 Event reconstruction and selection

The global event reconstruction (also called particle-flow event reconstruction [45]) reconstructs and identifies each individual particle in an event with an optimized combination of all subdetector information. In this process, the identification of the particle type (photon, electron, muon, charged hadron or neutral hadron) plays an important role in the determination of the particle direction and energy. Photons (e.g., coming from π^0 decays or from electron bremsstrahlung) are identified as ECAL energy clusters not linked to the extrapolation to the ECAL of any charged particle trajectory. Electrons are identified as a primary charged particle track with one or more ECAL energy clusters consistent with the extrapolation of this track to the ECAL or with bremsstrahlung photons emitted as the electron passes through the tracker material. Muons (e.g., from b-hadron semileptonic decays) are identified as a track in the central tracker consistent with either a track or several hits in the muon system, and associated with calorimeter deposits compatible with the muon hypothesis. Charged hadrons are identified as charged particle tracks that are not identified as electrons or muons. Finally, neutral hadrons are identified as either HCAL energy clusters not linked to any charged hadron trajectory or ECAL and HCAL energy excesses with respect to any expected charged hadron energy deposit.

The high instantaneous luminosity of the LHC results in multiple pp interactions per bunch crossing. The reconstructed vertex with the largest value of summed physics-object p_T^2 is the primary pp interaction vertex. The physics objects are the jets, clustered using the anti-k_T jet finding algorithm [46,47] with the tracks assigned to the vertex as inputs, and the associated missing p_T, taken as the negative vector p_T sum of those jets.

Photon and electron candidates are reconstructed by summing and clustering the energy deposits in the ECAL crystals. Groups of these clusters, called superclusters, are combined to recover the bremsstrahlung energy of electrons and converted photons passing through the tracker. In the endcaps, preshower energy is added in the region covered by the preshower ($1.65 < |\eta| < 2.60$). The clustering algorithms result in an almost complete recovery of the energy of photons.

A multivariate discriminant is used to identify photon candidates. The inputs to the discriminant are the isolation variables, the ratio of hadronic energy in the HCAL towers behind the superclusters to the electromagnetic energy in the superclusters, and the transverse width of the electromagnetic shower. A conversion-safe electron veto [26], which requires no charged-particle track with a hit in the inner layer of the pixel detector pointing to the photon cluster in the ECAL, is applied to avoid misidentifying an electron as a converted photon. Photons are required to be reconstructed within the region $|\eta| < 2.5$, although those in the ECAL transition region $1.44 < |\eta| < 1.57$ are excluded from the analysis. The efficiency of the photon identification procedure is measured with $Z \rightarrow ee$ events using "tag-and-probe" techniques [48], and is between 84–91 (77–94)%, depending on the transverse energy E_T, in the barrel (endcap). The electron veto efficiencies are measured with $Z \rightarrow \mu\mu\gamma$ events, where the photon is produced by final-state radiation, and found to be 98 (94)% in the barrel (endcap).

Muons are reconstructed by combining information from the silicon tracker and the muon system [49]. The matching between the inner and outer tracks proceeds either outside-in, starting from a track in the muon system, or inside-out, starting from a track in the silicon tracker. In the latter case, tracks that match track segments in only one or two planes of the muon system are also included in the analysis to ensure that very low-p_T muons that may not have sufficient energy to penetrate the entire muon system are retained. Muons reconstructed only in the muon system are not retained for the analysis. In order to avoid reconstructing a single muon as multiple muons, whenever two muons share more than half of their segments, the one with lower reconstruction quality is removed. The compatibility with a minimum ionizing particle signature expected in the calorimeters is taken into account [50]. Muons with $p_T > 4$ GeV and $|\eta| < 2.4$ are accepted.

To suppress muons originating from in-flight decays of hadrons, the impact parameter of each muon track, defined as its distance of closest approach to the primary event vertex position, is required to be less than 0.5 (1.0) cm in the transverse (longitudinal) plane. In addition, the three-dimensional impact parameter is required to be less than four times its uncertainty. A cone of size $\Delta R = \sqrt{(\Delta\phi)^2 + (\Delta\eta)^2} = 0.3$ is constructed around the momentum direction of each muon

candidate, where ϕ is the azimuthal angle in radians. The relative isolation variable for the muons is defined by summing the p_T of all photons, charged hadrons, and neutral hadrons within this cone, correcting for additional underlying event activity due to pileup events [51], and then dividing by the muon p_T:

$$
\mathcal{I}^\mu \equiv \Big(\sum p_T^{\text{charged}} \\
+ \max \Big[0, \sum p_T^{\text{neutral}} + \sum p_T^\gamma - p_T^{\text{PU}}(\mu) \Big] \Big) / p_T^\mu,
\tag{3}
$$

where $p_T^{\text{PU}}(\mu) \equiv 0.5 \sum_i p_T^{\text{PU},i}$, and i runs over the momenta of the charged-hadron particle-flow candidates not originating from the primary vertex. The $\sum p_T^{\text{charged}}$ is the scalar p_T sum of charged hadrons originating from the primary event vertex. The $\sum p_T^{\text{neutral}}$ and $\sum p_T^\gamma$ are the scalar p_T sums of neutral hadrons and photons, respectively. The requirement $\mathcal{I}^\mu < 0.35$ is imposed on the leading muon to reject muons from electroweak decays of hadrons within jets or any jets that punch through the calorimeters mimicking a muon signature. The angular separation ΔR between the two muons is small because of their low invariant mass, $m_{\mu\mu}$, and the high p_T of the J/ψ meson from the decay of the Z or Higgs boson. Therefore, no isolation requirement is applied to the subleading muons since they are within the isolation cone of the leading muon in most events. The momentum of the subleading muon is excluded from the isolation calculation. The efficiency of identification is measured in $Z \rightarrow \mu\mu$ and J/$\psi \rightarrow \mu\mu$ events using the tag-and-probe method, and is 94–98 (92–97)% in the barrel (endcap), depending on muon p_T and η. The isolation efficiency, which is p_T dependent, is measured to be 90–100 (92–100)% in the barrel (endcap), and is consistent with the measurement from $Z \rightarrow \mu\mu$ events.

Signal candidates are selected by applying additional selection criteria to events containing at least two muons and one photon. The two muons must have opposite charges and $p_T > 20$ (4) GeV for the leading (subleading) muon. The p_T requirement for the leading muon is driven by the trigger threshold. The requirement that the photon has $E_T > 33$ GeV is also driven by the trigger threshold. The angular separation of each muon from the photon is required to satisfy $\Delta R > 1$ in order to suppress Drell-Yan background events with final-state radiation. To ensure that the dimuon J/ψ candidate is well-separated from the photon, events are required to have $\Delta R(\mu\mu, \gamma) > 2$ and $|\Delta\phi(\mu\mu, \gamma)| > 1.5$. Both the photon and dimuon momenta must satisfy $p_T/m_{\mu\mu\gamma} > 0.38$ (0.28) for the Z (H) boson decay. This constraint helps to reject the γ^*+jet and γ+jet backgrounds, with minimal effect on the signal efficiency and $m_{\mu\mu\gamma}$ spectrum. Events in which the mass of the two muons is consistent with the mass of the J/ψ meson [29], $3.0 < m_{\mu\mu} < 3.2$ GeV, are retained. In addition,

Table 1 The number of observed Z or H boson events, the expected signal yields, the expected nonresonant background with uncertainties estimated from the fit (described in Sect. 5), and the expected reso- nant background (see Sect. 3) contribution in the ranges of 81 or 120 $< m_{\mu\mu\gamma} <$ 101 or 130 GeV, respectively, for the Z or H boson searches

$Z \to J/\psi\gamma$ (81 $< m_{\mu\mu\gamma} <$ 101 GeV)					$H \to J/\psi\gamma$ (120 $< m_{\mu\mu\gamma} <$ 130 GeV)				
Category	Observed data	Signal	Nonresonant background	Resonant background	Category	Observed data	Signal	Nonresonant background	Resonant background
EB high R_9	69	0.69	66.9 ± 4.9	2.1					
EB low R_9	67	0.42	62.6 ± 4.6	1.2	Inclusive	56	0.076	51.0 ± 3.4	0.20
EE	47	0.30	43.0 ± 4.0	1.0					

only events with a three-body invariant mass in the range of 70 (100) $< m_{\mu\mu\gamma} <$ 120 (150) GeV are considered in the Z (H) boson search.

The simulated events are reconstructed using the same algorithms as the data, but the simulation does not reproduce the data perfectly. The differences in efficiencies between data and simulation for trigger, offline object reconstruction, identification, and isolation are corrected by reweighting the simulated events with data-to-simulation correction factors. The scale correction factors are observed to deviate from 1 by less than 2.5%. The energy and momentum resolutions for muons and photons in simulated events are also corrected to match those in $Z \to \mu\mu$/ee events in data.

In the $Z \to J/\psi\gamma$ search, selected events are classified into mutually exclusive categories in order to enhance the sensitivity of the search. The categorization is based on the η and R_9 variables of the photon, where R_9 is defined as the energy sum of 3×3 ECAL crystals centered on the most ener- getic crystal in the supercluster associated with the photon, divided by the energy of the supercluster [26]. Photons that do not convert to an e^+e^- pair in the detector tend to have high values of R_9 and a threshold of 0.94 is used to classify reconstructed photons with high R_9 (thus with a better reso- lution) and low R_9 (worse resolution). The three categories are: (1) photon in the barrel region with a high R_9 value (referred to as EB high R_9); (2) photon in the barrel region with low R_9 value (referred to as EB low R_9); and (3) photon in the endcap region (referred to as EE). The EE category is not divided into high/low R_9 because there are only a few events in this category. Events in the $H \to J/\psi\gamma$ search are not divided into categories since the sample size is limited and the sensitivity is still far from the SM prediction, and therefore event categorization does not result in a significant improvement in the expected limit.

Table 1 shows the numbers of observed events in data, the expected yields from the Z (H) $\to J/\psi\gamma$ signals, the expected nonresonant backgrounds with uncertainties esti- mated from the fits (described in Sect. 5), and the expected resonant background contributions in the range of 81 (120) $< m_{\mu\mu\gamma} <$ 101 (130) GeV for the Z (H) boson search. The

values for the signal yields quoted for the Z boson decay assume that the J/ψ meson is unpolarized and those for the Higgs boson decay assume transverse polarization for the J/ψ meson. In the Z and Higgs boson channels, the num- bers of events coming from the resonant backgrounds are large compared with those expected for the signal in the SM. However, the resonant backgrounds are small compared to the nonresonant backgrounds and therefore their effect on the final result is minimal.

The overall signal efficiency, including kinematic accep- tance, trigger, object reconstruction, identification, and isola- tion efficiencies for the J/$\psi\gamma \to \mu\mu\gamma$ final state, is approx- imately 14 (22)% for the Z (H) boson signal, respectively. The total signal efficiency for the Z boson decay is 13% if the J/ψ meson is fully transversely polarized and 16% if it is fully longitudinally polarized. The difference between the efficiency for the Z boson and that for the Higgs boson arises from the differences in the p_T spectra for the muons and the photon in the two cases. These differences are due to the difference between the Z boson and Higgs boson masses.

Figures 4 and 5 show the dimuon invariant mass and pho- ton E_T distributions for both Z and Higgs boson searches with events from all categories included. The number of events in the distributions from signal events is set to 40 (750) times the SM predicted yield for the Z (H) boson decay. The number of events in distributions in the resonant background samples is normalized to 5 (150) times the expected yield. The peak at the J/ψ mass in data shows that real J/ψ candidates are reconstructed and selected. These events come from inclusive quarkonium production; no simulation is available for this analysis so they cannot be included in the distributions. The background from $Z \to \mu\mu\gamma$ events, for which a proper sim- ulation exists, is much smaller than from inclusive quarko- nium production, and it is scaled to make it visible. Figure 6 shows the distribution of the proper decay time t, defined as $(m_{\mu\mu}/p_T^{\mu\mu})L_{xy}$, where L_{xy} is the distance between the primary event vertex and the common vertex of the muons in the transverse plane, for both Z and Higgs boson decays. These distributions are normalized to the number of selected events in data. The negative values come from the fact that
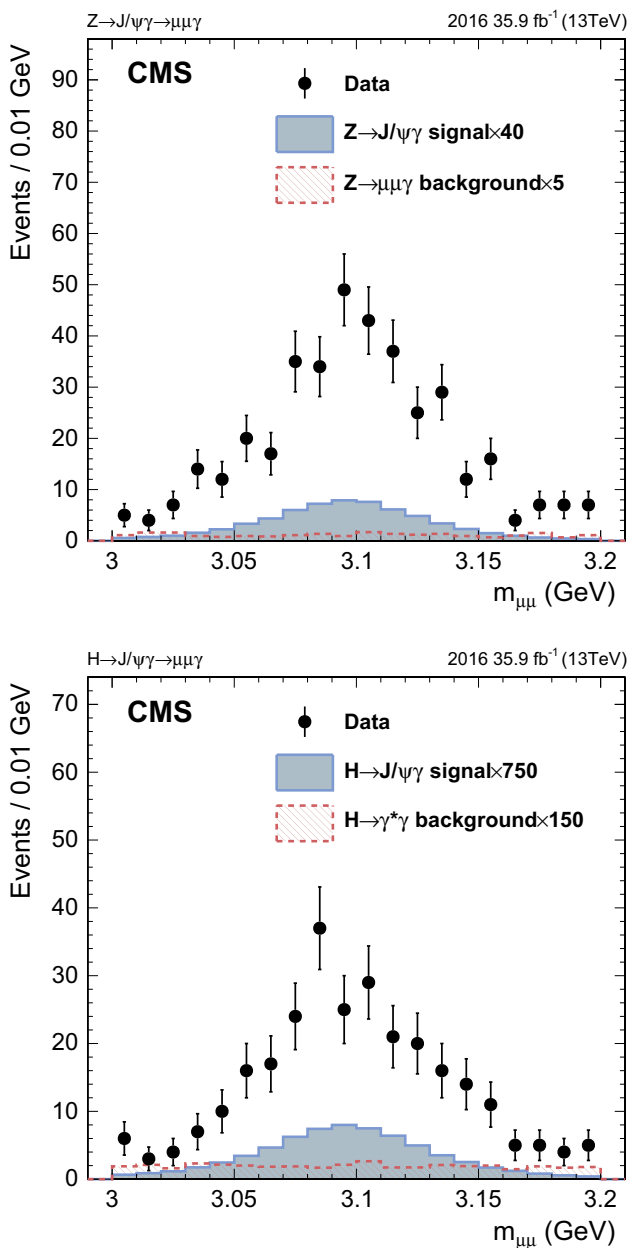
Fig. 4 The $m_{\mu\mu}$ distributions in the Z (upper) and Higgs (lower) boson searches. The number of events in the distributions from signal events is set to respective factors of 40 and 750 larger than the SM values for the predicted yields for Z and H boson decays. The number of events in distributions in the resonant background samples is normalized to 5 and 150 multiples in the expected yields

Fig. 5 The photon E_T distributions in the Z (upper) and Higgs (lower) boson searches. The number of events in the distributions from signal events is set to factors of 40 and 750 those of the SM predicted yields for the Z and H boson decays, respectively. The number of events in distributions in the resonant background samples is normalized to respective factors of 5 and 150 larger than the expected yields

L_{xy} is defined either to be positive or negative. The positive (negative) value indicates that the angle between the L_{xy} vector and the vector of $p_T^{J/\psi}$ is smaller (larger) than $\pi/2$. The distributions suggest that the J/ψ candidates reconstructed in data, like the signal events, are produced promptly at the pp interaction point, rather than coming from displaced heavy hadron decays.
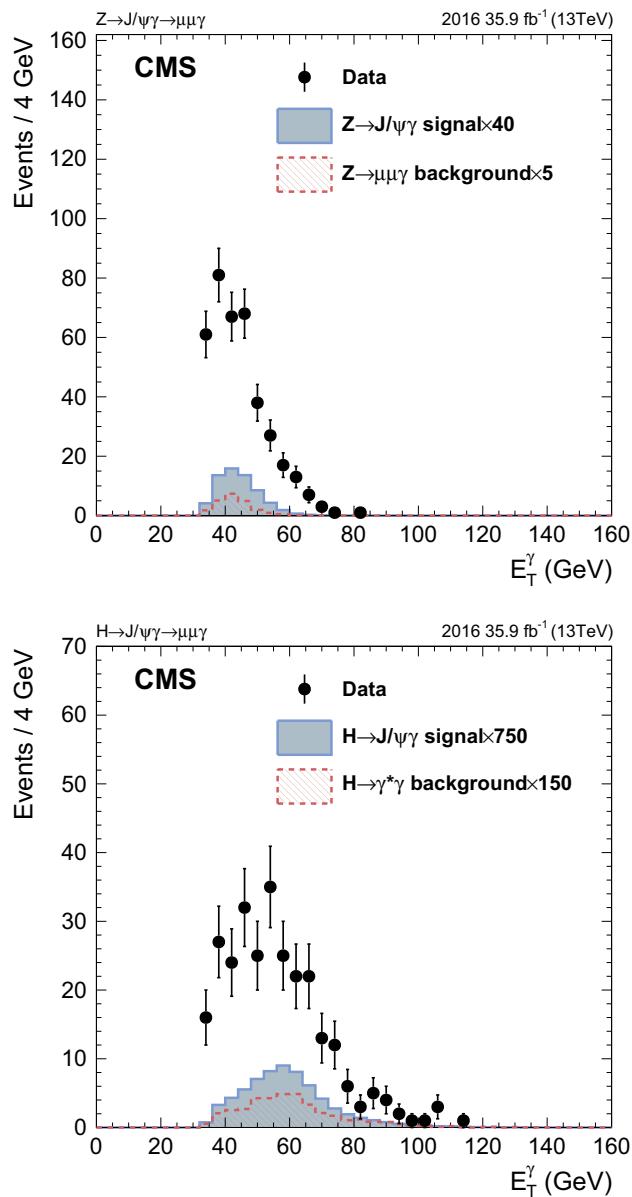
5 Background and signal modeling

The subdominant, resonant backgrounds are estimated from the simulated samples, while the continuum background for each category for both the Z and Higgs boson decays is estimated and modeled using data by fitting a parametric function to the $m_{\mu\mu\gamma}$ distribution. An unbinned maximum likelihood fit is performed over the range 70 (100) $< m_{\mu\mu\gamma} <$ 120 (150) GeV for the Z (H) $\rightarrow$ J/$\psi\gamma$ search. The true form
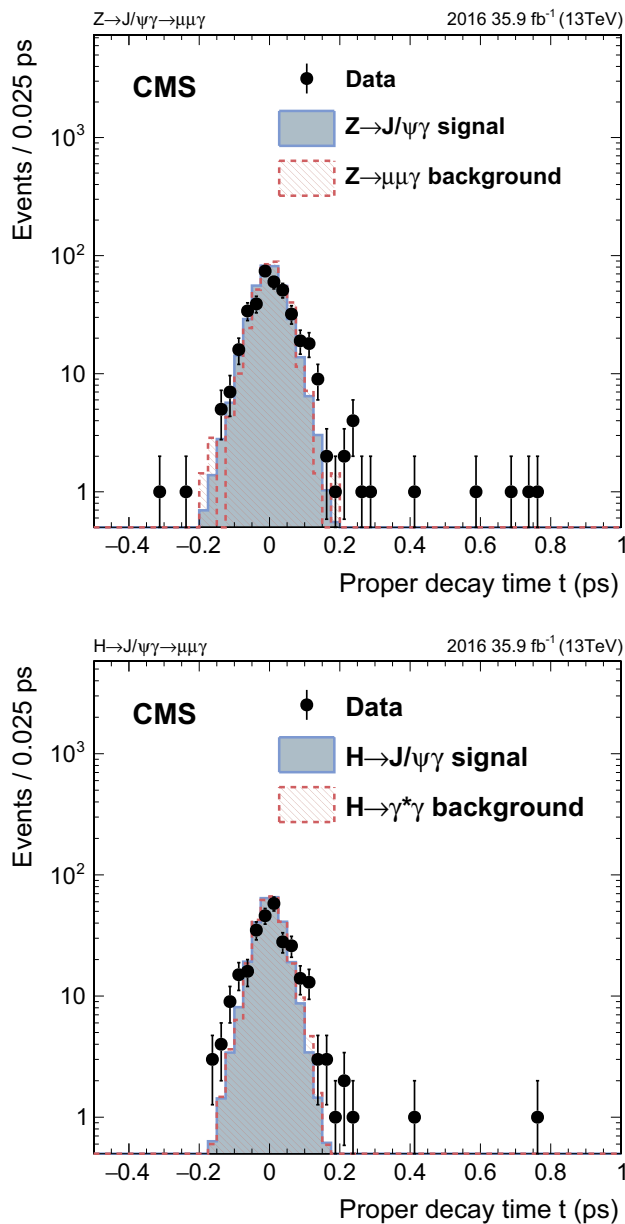
Fig. 6 The proper decay time, t, distributions in the Z (upper) and Higgs (lower) boson searches. Distributions in simulated events are normalized to the number of selected events in data. The distributions suggest that the J/ψ candidates reconstructed in data, just as signal events, are produced promptly at the pp interaction point, and not from displaced heavy-hadron decays

of the background $m_{\mu\mu\gamma}$ distribution is unknown and mismodeling of the background by the distribution obtained from the fit in data could lead to a bias in the analysis. The procedure used to study the bias introduced by the choice of function is described below.

Four families of functions are tested as potential parametrizations of the background: Bernstein polynomials, exponentials, power laws, and Laurent form polynomials. In the first step, one of the functions among the four families is chosen to fit the $m_{\mu\mu\gamma}$ distribution observed in data. Pseudo-events are randomly generated by using the resulting fit as a background model to simulate possible experiment results. Here, the order of the background function required to describe the data for each of the families is determined by increasing the number of parameters until an additional increase does not result in a significant improvement in the quality of the fit to the observed data. The improvement is quantified by the differences in the negative log-likelihood between fits with two consecutive orders of the same family of functions given the increment of the number of free parameters between two functions.

Signal events with signal strength μ_{gen} are introduced when generating the pseudo-events. The value $\mu_{\text{gen}} = 1$ corresponds to injecting 1 times the signal yield expected from the SM on top of the sum of resonant and nonresonant background. A fit is made to the distribution using one of the functions in the four families combined with a signal model, where the normalization of the signal in this step is allowed to be negative. This procedure is repeated 5000 times and for each of the functions, and it is expected that ideally on average the signal strength predicted by the fit μ_{fit} will be equal to μ_{gen}. The deviation of the mean fitted signal strength μ_{fit} from μ_{gen} in pseudo-events is used to quantify the potential bias. The criterion for the bias to be negligible is that the deviation must be at least five times smaller than the statistical uncertainty on μ_{fit}. In other words, the distribution of the pull values, defined as $(\mu_{\text{fit}} - \mu_{\text{gen}})/\sigma_{\text{fit}}$, calculated from each pseudo-event should have a mean value of less than 0.2. This requirement implies and ensures that the uncertainty in the frequentist coverage, defined as the fraction of experiments where the true value is contained within the confidence interval, is negligible.

The polynomial background function satisfies the bias requirement. An order-three polynomial function is used for each category in the Z boson search, and an order-two polynomial function is used in the Higgs boson search. The $m_{\mu\mu\gamma}$ distribution and background model for each category is shown in Fig. 7.

The signal model for each case is obtained from an unbinned maximum likelihood fit to the $m_{\mu\mu\gamma}$ distributions of the corresponding sample of simulated events. In the Z boson search, a double-sided Crystal Ball function [52] is used. A Crystal Ball function plus a Gaussian with the same mean value is used in the Higgs boson search.

6 Results

The distributions in $m_{\mu\mu\gamma}$ observed in the data are in agreement with the SM expectation of the background-only hypothesis. The results are used to derive upper limits on the branching fractions, $\mathcal{B}(Z \to J/\psi\gamma)$ and $\mathcal{B}(H \to J/\psi\gamma)$.
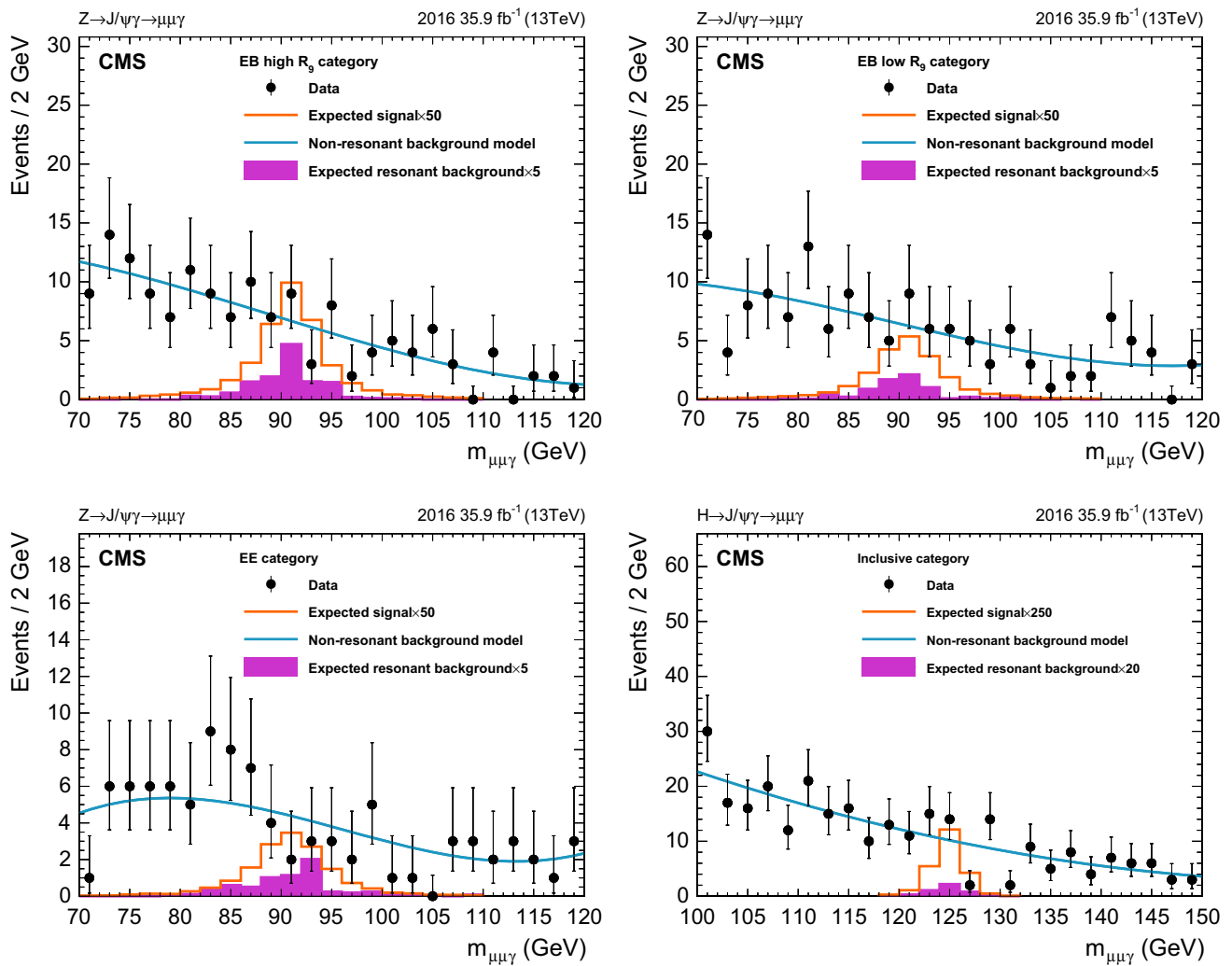
Fig. 7 Fits to nonresonant background using lowest-order unbiased functions to describe the three-body invariant mass $m_{\mu\mu\gamma}$ distributions observed in data for the Z $\rightarrow$ J/$\psi\gamma$ channel in the EB high R_9 category (top left), the EB low R_9 category (top right), the EE category (bottom left), as well as the H $\rightarrow$ J/$\psi\gamma$ channel (bottom right)

The exclusion limits are evaluated using the modified frequentist approach, CL$_s$, taking the profile likelihood as a test statistic [53–56]. An unbinned evaluation of the likelihood is performed.

Systematic uncertainties in the expected number of signal events and in the signal model used in the fit come from the imperfect simulation of the detector and uncertainties in the theoretical prediction for the signal production. They are evaluated by varying contributing sources within their corresponding uncertainties and propagating the uncertainties to the signal yields or shapes in simulated signal samples. The sources of the uncertainties and their magnitudes are summarized in Table 2. The uncertainties are classified into two types, one affecting the predicted signal yields and the other affecting the shapes of the signal models. The first type includes the uncertainties in the luminosity measurement [57], the pileup modeling in the simulations, the cor-

rections applied to the simulated events in order to compensate for differences in trigger, object reconstruction, and identification efficiencies, and the theoretical uncertainties. The theoretical uncertainties come from the effects of the PDF choice on the signal cross section [33,38,58], the lack of higher-order calculations for the cross-section [59–63], and the prediction of the decay branching fractions [64]. The second type arises from the uncertainties in the momentum (energy) scale and resolution for muons (photons). These uncertainties are incorporated into the signal models by varying the momentum (energy) scale and resolution and introducing the effects on the mean and width of the Gaussian component of the signal models as shape nuisance parameters in the estimation of the limits.

The systematic uncertainties associated with the resonant background processes are evaluated with the methods used for the signal samples. The continuum background prediction

Table 2 Systematic uncertainties in both the searches for Z → J/$\psi\gamma$ and H → J/$\psi\gamma$. In the Z → J/$\psi\gamma$ search, the uncertainties are averaged over all categories. The numbers for uncertainties in the integrated luminosity, theoretical uncertainties, detector simulation and reconstruction correspond to the changes in the expected number of signal and resonant background events. The numbers for the uncertainties in the signal model correspond to the effect on the mean and width of the Gaussian component of the signal models resulting from the object momentum resolutions

Source	Z → J/$\psi\gamma$ channel		H → J/$\psi\gamma$ channel	
	Signal	Resonant background	Signal	Resonant background
Integrated luminosity	2.5%			
Theoretical uncertainties				
Signal cross section (scale)	3.5%	5.0%	+4.6% − 6.7%	
Signal cross section (PDF)	1.7%	5.0%	3.2%	
Branching fraction	–	5.0%	–	6.0%
Detector simulation, reconstruction				
Pileup weight	0.8%	1.8%	0.7%	1.6%
Trigger	4.0%	4.0%	3.9%	4.0%
Muon ident./Isolation	3.0%	3.4%	2.0%	2.5%
Photon identification	1.1%	1.1%	1.2%	1.2%
Electron veto	1.1%	1.1%	1.0%	1.0%
Signal model				
$m_{\mu\mu\gamma}$ scale	0.06%	–	0.1%	–
$m_{\mu\mu\gamma}$ resolution	1.0%	–	4.8%	–

Table 3 Limits for Z and H decays to J/$\psi-> \mu\mu$ final states. Shown in the second and third columns are the observed and expected limits for cross sections and branching fractions, with the upper and lower bounds in the expected 68% CL intervals shown, respectively, as super-scripts and subscripts. The third column presents the Z decay branching fractions when the J/ψ is assumed to be produced with $\lambda_\theta = +1$ or -1, in the helicity frame

Channel	Polarization	σ (fb) at 95% CL	$\mathcal{B}$(Z (H) → J/$\psi\gamma$) at 95% CL	$\frac{\mathcal{B}(\text{Z (H)} \rightarrow \text{J}/\psi\gamma)}{\mathcal{B}_{\text{SM}}(\text{Z (H)} \rightarrow \text{J}/\psi\gamma)}$
Z → J/$\psi\gamma$	Unpolarized	4.6 ($5.3^{+2.3}_{-1.6}$)	1.4 ($1.6^{+0.7}_{-0.5}$) $\times 10^{-6}$	15 (18)
	Transverse	5.0 ($5.9^{+2.5}_{-1.7}$)	1.5 ($1.7^{+0.7}_{-0.5}$) $\times 10^{-6}$	16 (19)
H → J/$\psi\gamma$	Longitudinal	3.9 ($4.6^{+2.0}_{-1.4}$)	1.2 ($1.4^{+0.6}_{-0.4}$) $\times 10^{-6}$	13 (15)
	Transverse	2.5 ($1.7^{+0.8}_{-0.5}$)	7.6 ($5.2^{+2.4}_{-1.6}$) $\times 10^{-4}$	260 (170)

is derived solely from data, so only statistical uncertainties are considered, which are translated into the uncertainties in each parameter of the fit function. The bias study mentioned in the previous section is performed to ensure that the bias from the choice of the background function is negligible. Hence, no additional systematic uncertainty is assigned to that background estimate.

The observed and median expected exclusion limits on the production cross sections and branching fractions at 95% confidence level (CL) for the Z and Higgs boson searches are summarized in Table 3. With the assumption that the J/ψ meson is unpolarized, the observed upper limit on the branching fraction of Z → J/$\psi\gamma$ is 1.4×10^{-6}, whereas the median expected upper limit is $1.6^{+0.7}_{-0.5} \times 10^{-6}$ with the 68% CL interval indicated by the subscript and superscript. The observed and median expected limits correspond to 15 and 18 times the SM prediction, respectively. Extreme polarization scenarios give rise to variations from $-13.6(-13.5)$%, for a fully longitudinally polarized J/ψ, to $+8.6 (+8.2)$%, for a fully transversely polarized J/ψ meson, in the observed (expected)

branching fraction. The observed upper limit on the branching fraction of H → J/$\psi\gamma$ is 7.6×10^{-4}, and the median expected upper limit is $5.2^{+2.4}_{-1.6} \times 10^{-4}$. The observed and median expected limits correspond to 260 and 170 times the SM prediction. For the Higgs boson decay, the J/ψ is assumed to be fully transversely polarized. The overall impact of systematic uncertainties in the final results is negligible.

The results from our H → J/$\psi\gamma$ analysis are combined with the results from a similar search performed by the CMS Collaboration using pp collision data at $\sqrt{s} = 8$ TeV, corresponding to an integrated luminosity of 19.7 fb^{-1} [20]. The combination results in an upper limit corresponding to 220 (160) times the SM prediction. The uncertainties are assumed either uncorrelated or correlated; the difference in the result is negligible.

7 Summary

A search is performed for decays of the standard model (SM) Z and Higgs bosons into a J/ψ meson and a photon, with the

J/ψ meson subsequently decaying into $\mu^+\mu^-$. The data are from pp collisions at $\sqrt{s} = 13$ TeV, corresponding to an integrated luminosity of $35.9\,\mathrm{fb}^{-1}$. No excess is observed above the measured background. The observed and expected exclusion limits at 95% confidence level (CL) on the branching fraction of the Z boson decay in the unpolarized case are $\mathcal{B}(Z \rightarrow J/\psi\,\gamma) < 1.4$ and $1.6^{+0.7}_{-0.5} \times 10^{-6}$, corresponding to factors of 15 and 18 greater than the SM prediction. The 68% CL range in the confidence interval is shown as the subscript and superscript. Extreme polarization possibilities give rise to changes from -13.6 and -13.5% for a longitudinally polarized J/ψ meson, to $+8.6$ and $+8.2\%$, for a transversely polarized J/ψ meson, in the respective observed and expected branching fractions. The 95% CL limit on the branching fraction of the Higgs boson are $\mathcal{B}(H \rightarrow J/\psi\,\gamma) < 7.6$ and $5.2^{+2.4}_{-1.6} \times 10^{-4}$, corresponding to factors of 260 and 170 times the SM value. The results for the Higgs boson channel are combined with previous CMS data from proton-proton collisions at $\sqrt{s} = 8$ TeV to produce observed and expected upper limits on the branching fraction for the decay $H \rightarrow J/\psi\,\gamma$ of factors of 220 and 160 larger than the SM predictions.

References

1. ATLAS Collaboration, Observation of a new particle in the search for the standard model Higgs boson with the ATLAS detector at the LHC. Phys. Lett. B **716**, 1 (2012). https://doi.org/10.1016/j.physletb.2012.08.020. arXiv:1207.7214

2. ATLAS Collaboration, Evidence for the spin-0 nature of the Higgs boson using ATLAS data. Phys. Lett. B **726**, 120 (2013). https://doi.org/10.1016/j.physletb.2013.08.026. arXiv:1307.1432

3. CMS Collaboration, Observation of a new boson at a mass of 125 GeV with the CMS experiment at the LHC. Phys. Lett. B **716**, 30 (2012). https://doi.org/10.1016/j.physletb.2012.08.021. arXiv:1207.7235

4. CMS Collaboration, Observation of a new boson with mass near 125 GeV in pp collisions at $\sqrt{s} = 7$ and 8 TeV. JHEP **06**, 081 (2013). https://doi.org/10.1007/JHEP06(2013)081. arXiv:1303.4571

5. CMS Collaboration, Precise determination of the mass of the Higgs boson and tests of compatibility of its couplings with the standard model predictions using proton collisions at 7 and 8 TeV. Eur. Phys. J. C **75**, 212 (2015). https://doi.org/10.1140/epjc/s10052-015-3351-7. arXiv:1412.8662

6. ATLAS Collaboration, Measurements of the Higgs boson production and decay rates and coupling strengths using pp collision data at $\sqrt{s} = 7$ and 8 TeV in the ATLAS experiment. Eur. Phys. J. C **76** (2016). https://doi.org/10.1140/epjc/s10052-015-3769-y. arXiv:1507.04548

7. ATLAS and C. Collaborations, Measurements of the Higgs boson production and decay rates and constraints on its couplings from

a combined ATLAS and CMS analysis of the LHC pp collision data at $\sqrt{s} = 7$ and 8 TeV. JHEP **08**, 45 (2016). https://doi.org/10.1007/JHEP08(2016)045. arXiv:1606.02266

8. G.T. Bodwin, F. Petriello, S. Stoynev, M. Velasco, Higgs boson decays to quarkonia and the H$c\bar{c}$ coupling. Phys. Rev. D **88**, 053003 (2013). https://doi.org/10.1103/PhysRevD.88.053003. arXiv:1306.5770

9. B. Guberina, J.H. Kühn, R.D. Peccei, R. Rückl, Rare decays of the Z^0. Nucl. Phys. B **174**, 317 (1980). https://doi.org/10.1016/0550-3213(80)90287-4

10. T.-C. Huang, F. Petriello, Rare exclusive decays of the Z boson revisited. Phys. Rev. D **92**, 014007 (2015). https://doi.org/10.1103/PhysRevD.92.014007. arXiv:1411.5924

11. Y. Grossman, M. König, M. Neubert, Exclusive radiative decays of W and Z bosons in QCD factorization. JHEP **04**, 101 (2015). https://doi.org/10.1007/JHEP04(2015)101. arXiv:1501.06569

12. G.T. Bodwin, H.S. Chung, J.-H. Ee, J. Lee, Z-boson decays to a vector quarkonium plus a photon. Phys. Rev. D **97**, 016009 (2018). https://doi.org/10.1103/PhysRevD.97.016009. arXiv:1709.09320

13. G. T. Bodwin, H. S. Chung, J.-H. Ee, and J. Lee, Addendum: New approach to the resummation of logarithms in Higgs-boson decays to a vector quarkonium plus a photon [Phys. Rev. D 95 (2017) 054018]. Phys. Rev. D **96**, 116014 (2017). https://doi.org/10.1103/PhysRevD.96.116014. arXiv:1710.09872

14. C. Delaunay, T. Golling, G. Perez, Y. Soreq, Enhanced Higgs boson coupling to charm pairs. Phys. Rev. D **89**, 033014 (2014). https://doi.org/10.1103/PhysRevD.89.033014. arXiv:1310.7029

15. M. Trott, M.B. Wise, On theories of enhanced CP violation in B$_{s,d}$ meson mixing. JHEP **11**, 157 (2010). https://doi.org/10.1007/JHEP11(2010)157. arXiv:1009.2813

16. M. Jung, A. Pich, P. Tuzon, Charged-Higgs phenomenology in the aligned two-Higgs-doublet model. JHEP **11**, 003 (2010). https://doi.org/10.1007/JHEP11(2010)003. arXiv:1006.0470

17. G.F. Giudice, C. Grojean, A. Pomarol, R. Rattazzi, The strongly-interacting light Higgs. JHEP **06**, 045 (2007). https://doi.org/10.1088/1126-6708/2007/06/045. arXiv:hep-ph/0703164

18. C. Delaunay et al., Light nondegenerate composite partners at the LHC. JHEP **02**, 055 (2014). https://doi.org/10.1007/JHEP02(2014)055. arXiv:1311.2072

19. ATLAS Collaboration, Search for Higgs and Z boson decays to J/$\psi\gamma$ and Υ(nS)γ with the ATLAS detector. Phys. Rev. Lett. **114**, 121801 (2015). https://doi.org/10.1103/PhysRevLett.114.121801. arXiv:1501.03276

20. C.M.S. Collaboration, Search for a Higgs boson decaying into $\gamma^*\gamma \rightarrow \ell\ell\gamma$ with low dilepton mass in pp collisions at $\sqrt{s} = $ 8 TeV. Phys. Lett. B **753**, 341 (2016). https://doi.org/10.1016/j.physletb.2015.12.039. arXiv:1507.03031

21. ATLAS Collaboration, Searches for exclusive Higgs and Z boson decays into J/$\psi\gamma$, ψ(2S)γ, and Υ(nS)γ at $\sqrt{s} = $ 13 TeV with the ATLAS detector. Phys. Lett. B **786**, 134 (2018). https://doi.org/10.1016/j.physletb.2018.09.024. arXiv:1807.00802

22. ATLAS Collaboration, Search for the decay of the Higgs boson to charm quarks with the ATLAS experiment. Phys. Rev. Lett. **120**, 211802 (2018). https://doi.org/10.1103/PhysRevLett.120.211802. arXiv:1802.04329

23. CMS Collaboration, The CMS experiment at the CERN LHC. JINST **3**, S08004 (2008). https://doi.org/10.1088/1748-0221/3/08/S08004

24. CMS Collaboration, Description and performance of track and primary-vertex reconstruction with the CMS tracker. JINST **9**, P10009 (2014). https://doi.org/10.1088/1748-0221/9/10/P10009. arXiv:1405.6569

25. CMS Collaboration, Performance of electron reconstruction and selection with the CMS detector in proton-proton collisions at $\sqrt{s} = $ 8 TeV. JINST **10**, P06005 (2015). https://doi.org/10.1088/1748-0221/10/06/P06005. arXiv:1502.02701

26. CMS Collaboration, Performance of photon reconstruction and identification with the CMS detector in proton-proton collisions at $\sqrt{s} = $ 8 TeV. JINST **10**, P08010 (2015). https://doi.org/10.1088/1748-0221/10/08/P08010. arXiv:1502.02702

27. CMS Collaboration, Performance of the CMS muon detector and muon reconstruction with proton-proton collisions at $\sqrt{s} = $ 13 TeV. JINST **13**, P06015 (2018). https://doi.org/10.1088/1748-0221/13/06/P06015. arXiv:1804.04528

28. CMS Collaboration, The CMS trigger system. JINST **12**, P01020 (2017). https://doi.org/10.1088/1748-0221/12/01/P01020. arXiv:1609.02366

29. Particle Data Group, M. Tanabashi et al., Review of particle physics. Phys. Rev. D **98**, 030001 (2018). https://doi.org/10.1103/PhysRevD.98.030001

30. T. Sjöstrand, S. Mrenna, P .Z. Skands, A brief introduction to PYTHIA 8.1. Comput. Phys. Commun. **178**, 852 (2008). https://doi.org/10.1016/j.cpc.2008.01.036. arXiv:0710.3820

31. T. Sjöstrand et al., An introduction to PYTHIA 8.2. Comput. Phys. Commun. **191**, 159 (2015). https://doi.org/10.1016/j.cpc.2015.01.024. arXiv:1410.3012

32. CMS Collaboration, Event generator tunes obtained from underlying event and multiparton scattering measurements. Eur. Phys. J. C **76**, 155 (2016). https://doi.org/10.1140/epjc/s10052-016-3988-x. arXiv:1512.00815

33. NNPDF Collaboration, Parton distributions for the LHC Run II. JHEP **04**, 040 (2015). https://doi.org/10.1007/JHEP04(2015)040. arXiv:1410.8849

34. Y. Li, F. Petriello, Combining QCD and electroweak corrections to dilepton production in FEWZ. Phys. Rev. D **86**, 094034 (2012). https://doi.org/10.1103/PhysRevD.86.094034. arXiv:1208.5967

35. S. Alioli, P. Nason, C. Oleari, E. Re, NLO Higgs boson production via gluon fusion matched with shower in POWHEG. JHEP **04**, 002 (2009). https://doi.org/10.1088/1126-6708/2009/04/002. arXiv:0812.0578

36. P. Nason, C. Oleari, NLO Higgs boson production via vector-boson fusion matched with shower in POWHEG. JHEP **02**, 037 (2010). https://doi.org/10.1007/JHEP02(2010)037. arXiv:0911.5299

37. J. Alwall et al., The automated computation of tree-level and next-to-leading order differential cross sections, and their matching to parton shower simulations. JHEP **07**, 079 (2014). https://doi.org/10.1007/JHEP07(2014)079. arXiv:1405.0301

38. LHC Higgs Cross Section Working Group Collaboration, Handbook of LHC Higgs cross sections: 4. Deciphering the nature of the Higgs sector. (2016). arXiv:1610.07922

39. S. Palestini, Angular distribution and rotations of frame in vector meson decays into lepton pairs. Phys. Rev. D **83**, 031503 (2011). https://doi.org/10.1103/PhysRevD.83.031503. arXiv:1012.2485

40. CMS Collaboration, Angular coefficients of Z bosons produced in pp collisions at $\sqrt{s} = $ 8 TeV and decaying to $\mu^+\mu^-$ as a function of transverse momentum and rapidity. Phys. Lett. B **750**, 154 (2015). https://doi.org/10.1016/j.physletb.2015.08.061. arXiv:1504.03512

41. ATLAS Collaboration, Measurement of the angular coefficients in Z-boson events using electron and muon pairs from data taken at $\sqrt{s} = $ 8 TeV with the ATLAS detector. JHEP **08**, 159 (2016). https://doi.org/10.1007/JHEP08(2016)159. arXiv:1606.00689

42. A. Abbasabadi, D. Bowser-Chao, D.A. Dicus, W.W. Repko, Radiative Higgs boson decays H $\rightarrow$ $f f \gamma$. Phys. Rev. D **55**, 5647 (1997). https://doi.org/10.1103/PhysRevD.55.5647. arXiv:hep-ph/9611209

43. J.M. Campbell, R. Ellis, MCFM for the Tevatron and the LHC. Nucl. Phys. Proc. Suppl. **205**, 10 (2010). https://doi.org/10.1016/j.nuclphysbps.2010.08.011. arXiv:1007.3492

44. GEANT4 Collaboration, Geant4—a simulation toolkit. Nucl. Instrum. Meth. A **506**, 250 (2003). https://doi.org/10.1016/S0168-9002(03)01368-8

45. C.M.S. Collaboration, Particle-flow reconstruction and global event description with the CMS detector. JINST **12**, P10003 (2017). https://doi.org/10.1088/1748-0221/12/10/P10003. arXiv:1706.04965

46. M. Cacciari, G.P. Salam, G. Soyez, The anti-k_T jet clustering algorithm. JHEP **04**, 063 (2008). https://doi.org/10.1088/1126-6708/2008/04/063. arXiv:0802.1189

47. M. Cacciari, G.P. Salam, G. Soyez, FastJet user manual. Eur. Phys. J. C **72**, 1896 (2012). https://doi.org/10.1140/epjc/s10052-012-1896-2. arXiv:1111.6097

48. CMS Collaboration, Measurement of the inclusive W and Z production cross sections in pp collisions at $\sqrt{s} = 7$ TeV. JHEP **10**, 132 (2011). https://doi.org/10.1007/JHEP10(2011)132. arXiv:1107.4789

49. CMS Collaboration, Performance of CMS muon reconstruction in pp collision events at $\sqrt{s} = 7$ TeV. JINST **7**, P10002 (2012). https://doi.org/10.1088/1748-0221/7/10/P10002. arXiv:1206.4071

50. CMS Collaboration, Measurements of properties of the Higgs boson decaying into the four-lepton final state in pp collisions at $\sqrt{s} = 13$ TeV. JHEP **11**, 047 (2017). https://doi.org/10.1007/JHEP11(2017)047. arXiv:1706.09936

51. CMS Collaboration, Search for neutral Higgs bosons decaying to tau pairs in pp collisions at $\sqrt{s} = 7$ TeV. Phys. Lett. B **713**, 68 (2012). https://doi.org/10.1016/j.physletb.2012.05.028. arXiv:1202.4083

52. M. J. Oreglia, A study of the reactions $\psi' \rightarrow \gamma\gamma\psi$. PhD Thesis, Stanford University, 1980. SLAC Report SLAC-R-236, see Appendix D

53. T. Junk, Confidence level computation for combining searches with small statistics. Nucl. Instrum. Meth. A **434**, 435 (1999). https://doi.org/10.1016/S0168-9002(99)00498-2. arXiv:hep-ex/9902006

54. A.L. Read, Presentation of search results: The CL$_s$ technique. J. Phys. G **28**, 2693 (2002). https://doi.org/10.1088/0954-3899/28/10/313

55. ATLAS and CMS Collaborations, The LHC Higgs combination group, Procedure for the LHC Higgs boson search combination in summer 2011. Technical Report CMS-NOTE-2011-005. ATL-PHYS-PUB-2011-11, 2011

56. G. Cowan, K. Cranmer, E. Gross, O. Vitells, Asymptotic formulae for likelihood-based tests of new physics. Eur. Phys. J. C **71**, 1554 (2011). https://doi.org/10.1140/epjc/s10052-011-1554-0. arXiv:1007.1727. [Erratum: 10.1140/epjc/s10052-013-2501-z]

57. CMS Collaboration, CMS luminosity measurements for the 2016 data taking period. CMS Physics Analysis Summary CMS-PAS-LUM-17-001, 2017

58. J. Butterworth et al., PDF4LHC recommendations for LHC Run II. J. Phys. G **43**, 023001 (2016). https://doi.org/10.1088/0954-3899/43/2/023001. arXiv:1510.03865

59. A.D. Martin, W.J. Stirling, R.S. Thorne, G. Watt, Parton distributions for the LHC. Eur. Phys. J. C **63**, 189 (2009). https://doi.org/10.1140/epjc/s10052-009-1072-5. arXiv:0901.0002

60. H. Lai et al., New parton distributions for collider physics. Phys. Rev. D **82**, 74024 (2010). https://doi.org/10.1103/PhysRevD.82.074024. arXiv:1007.2241

61. S. Alekhin et al., The PDF4LHC Working Group Interim Report. (2011). arXiv:1101.0536

62. M. Botje et al., The PDF4LHC Working Group Interim Recommendations. (2011). arXiv:1101.0538

63. R.D. Ball et al., Impact of heavy quark masses on parton distributions and LHC phenomenology. Nucl. Phys. B **849**, 296 (2011). https://doi.org/10.1016/j.nuclphysb.2011.03.021. arXiv:1101.1300

64. G. Passarino, Higgs boson production and decay: Dalitz sector. Phys. Lett. B **727**, 424 (2013). https://doi.org/10.1016/j.physletb.2013.10.052. arXiv:1308.0422

CMS Collaboration

Yerevan Physics Institute, Yerevan, Armenia
A. M. Sirunyan, A. Tumasyan

Institut für Hochenergiephysik, Wien, Austria
W. Adam, F. Ambrogi, E. Asilar, T. Bergauer, J. Brandstetter, M. Dragicevic, J. Erö, A. Escalante Del Valle, M. Flechl, R. Frühwirth[1], V. M. Ghete, J. Hrubec, M. Jeitler[1], N. Krammer, I. Krätschmer, D. Liko, T. Madlener, I. Mikulec, N. Rad, H. Rohringer, J. Schieck[1], R. Schöfbeck, M. Spanring, D. Spitzbart, A. Taurok, W. Waltenberger, J. Wittmann, C.-E. Wulz[1], M. Zarucki

Institute for Nuclear Problems, Minsk, Belarus
V. Chekhovsky, V. Mossolov, J. Suarez Gonzalez

Universiteit Antwerpen, Antwerpen, Belgium
E. A. De Wolf, D. Di Croce, X. Janssen, J. Lauwers, M. Pieters, H. Van Haevermaet, P. Van Mechelen, N. Van Remortel

Vrije Universiteit Brussel, Brussel, Belgium
S. Abu Zeid, F. Blekman, J. D'Hondt, I. De Bruyn, J. De Clercq, K. Deroover, G. Flouris, D. Lontkovskyi, S. Lowette, I. Marchesini, S. Moortgat, L. Moreels, Q. Python, K. Skovpen, S. Tavernier, W. Van Doninck, P. Van Mulders, I. Van Parijs

Université Libre de Bruxelles, Bruxelles, Belgium
D. Beghin, B. Bilin, H. Brun, B. Clerbaux, G. De Lentdecker, H. Delannoy, B. Dorney, G. Fasanella, L. Favart, R. Goldouzian, A. Grebenyuk, A. K. Kalsi, T. Lenzi, J. Luetic, N. Postiau, E. Starling, L. Thomas, C. Vander Velde, P. Vanlaer, D. Vannerom, Q. Wang

Ghent University, Ghent, Belgium
T. Cornelis, D. Dobur, A. Fagot, M. Gul, I. Khvastunov[2], D. Poyraz, C. Roskas, D. Trocino, M. Tytgat, W. Verbeke,
B. Vermassen, M. Vit, N. Zaganidis

Université Catholique de Louvain, Louvain-la-Neuve, Belgium
H. Bakhshiansohi, O. Bondu, S. Brochet, G. Bruno, C. Caputo, P. David, C. Delaere, M. Delcourt, A. Giammanco,
G. Krintiras, V. Lemaitre, A. Magitteri, A. Mertens, M. Musich, K. Piotrzkowski, A. Saggio, M. Vidal Marono, S. Wertz,
J. Zobec

Centro Brasileiro de Pesquisas Fisicas, Rio de Janeiro, Brazil
F. L. Alves, G. A. Alves, M. Correa Martins Jr., G. Correia Silva, C. Hensel, A. Moraes, M. E. Pol, P. Rebello Teles

Universidade do Estado do Rio de Janeiro, Rio de Janeiro, Brazil
E. Belchior Batista Das Chagas, W. Carvalho, J. Chinellato[3], E. Coelho, E. M. Da Costa, G. G. Da Silveira[4],
D. De Jesus Damiao, C. De Oliveira Martins, S. Fonseca De Souza, H. Malbouisson, D. Matos Figueiredo,
M. Melo De Almeida, C. Mora Herrera, L. Mundim, H. Nogima, W. L. Prado Da Silva, L. J. Sanchez Rosas, A. Santoro,
A. Sznajder, M. Thiel, E. J. Tonelli Manganote[3], F. Torres Da Silva De Araujo, A. Vilela Pereira

Universidade Estadual Paulista[a], Universidade Federal do ABC[b], São Paulo, Brazil
S. Ahuja[a], C. A. Bernardes[a], L. Calligaris[a], T. R. Fernandez Perez Tomei[a], E. M. Gregores[b], P. G. Mercadante[b],
S. F. Novaes[a], Sandra S. Padula[a]

Institute for Nuclear Research and Nuclear Energy, Bulgarian Academy of Sciences, Sofia, Bulgaria
A. Aleksandrov, R. Hadjiiska, P. Iaydjiev, A. Marinov, M. Misheva, M. Rodozov, M. Shopova, G. Sultanov

University of Sofia, Sofia, Bulgaria
A. Dimitrov, L. Litov, B. Pavlov, P. Petkov

Beihang University, Beijing, China
W. Fang[5], X. Gao[5], L. Yuan

Institute of High Energy Physics, Beijing, China
M. Ahmad, J. G. Bian, G. M. Chen, H. S. Chen, M. Chen, Y. Chen, C. H. Jiang, D. Leggat, H. Liao, Z. Liu, F. Romeo,
S. M. Shaheen[6], A. Spiezia, J. Tao, Z. Wang, E. Yazgan, H. Zhang, S. Zhang[6], J. Zhao

State Key Laboratory of Nuclear Physics and Technology, Peking University, Beijing, China
Y. Ban, G. Chen, A. Levin, J. Li, L. Li, Q. Li, Y. Mao, S. J. Qian, D. Wang, Z. Xu

Tsinghua University, Beijing, China
Y. Wang

Universidad de Los Andes, Bogota, Colombia
C. Avila, A. Cabrera, C. A. Carrillo Montoya, L. F. Chaparro Sierra, C. Florez, C. F. González Hernández,
M. A. Segura Delgado

University of Split, Faculty of Electrical Engineering, Mechanical Engineering and Naval Architecture, Split, Croatia
B. Courbon, N. Godinovic, D. Lelas, I. Puljak, T. Sculac

University of Split, Faculty of Science, Split, Croatia
Z. Antunovic, M. Kovac

Institute Rudjer Boskovic, Zagreb, Croatia
V. Brigljevic, D. Ferencek, K. Kadija, B. Mesic, A. Starodumov[7], T. Susa

University of Cyprus, Nicosia, Cyprus
M. W. Ather, A. Attikis, M. Kolosova, G. Mavromanolakis, J. Mousa, C. Nicolaou, F. Ptochos, P. A. Razis, H. Rykaczewski

Charles University, Prague, Czech Republic
M. Finger[8], M. Finger Jr.[8]

Escuela Politecnica Nacional, Quito, Ecuador
E. Ayala

Universidad San Francisco de Quito, Quito, Ecuador
E. Carrera Jarrin

Academy of Scientific Research and Technology of the Arab Republic of Egypt, Egyptian Network of High Energy Physics, Cairo, Egypt
M. A. Mahmoud[9,10], A. Mahrous[11], Y. Mohammed[9]

National Institute of Chemical Physics and Biophysics, Tallinn, Estonia
S. Bhowmik, A. Carvalho Antunes De Oliveira, R. K. Dewanjee, K. Ehataht, M. Kadastik, M. Raidal, C. Veelken

Department of Physics, University of Helsinki, Helsinki, Finland
P. Eerola, H. Kirschenmann, J. Pekkanen, M. Voutilainen

Helsinki Institute of Physics, Helsinki, Finland
J. Havukainen, J. K. Heikkilä, T. Järvinen, V. Karimäki, R. Kinnunen, T. Lampén, K. Lassila-Perini, S. Laurila, S. Lehti, T. Lindén, P. Luukka, T. Mäenpää, H. Siikonen, E. Tuominen, J. Tuominiemi

Lappeenranta University of Technology, Lappeenranta, Finland
T. Tuuva

IRFU, CEA, Université Paris-Saclay, Gif-sur-Yvette, France
M. Besancon, F. Couderc, M. Dejardin, D. Denegri, J. L. Faure, F. Ferri, S. Ganjour, A. Givernaud, P. Gras, G. Hamel de Monchenault, P. Jarry, C. Leloup, E. Locci, J. Malcles, G. Negro, J. Rander, A. Rosowsky, M. Ö. Sahin, M. Titov

Laboratoire Leprince-Ringuet, Ecole polytechnique, CNRS/IN2P3, Université Paris-Saclay, Palaiseau, France
A. Abdulsalam[12], C. Amendola, I. Antropov, F. Beaudette, P. Busson, C. Charlot, R. Granier de Cassagnac, I. Kucher, A. Lobanov, J. Martin Blanco, C. Martin Perez, M. Nguyen, C. Ochando, G. Ortona, P. Paganini, P. Pigard, J. Rembser, R. Salerno, J. B. Sauvan, Y. Sirois, A. G. Stahl Leiton, A. Zabi, A. Zghiche

Université de Strasbourg, CNRS, IPHC UMR 7178, Strasbourg, France
J.-L. Agram[13], J. Andrea, D. Bloch, J.-M. Brom, E. C. Chabert, V Cherepanov, C. Collard, E. Conte[13], J.-C. Fontaine[13], D. Gelé, U. Goerlach, M. Jansová, A.-C. Le Bihan, N. Tonon, P. Van Hove

Centre de Calcul de l'Institut National de Physique Nucleaire et de Physique des Particules, CNRS/IN2P3, Villeurbanne, France
S. Gadrat

Université de Lyon, Université Claude Bernard Lyon 1, CNRS-IN2P3, Institut de Physique Nucléaire de Lyon, Villeurbanne, France
S. Beauceron, C. Bernet, G. Boudoul, N. Chanon, R. Chierici, D. Contardo, P. Depasse, H. El Mamouni, J. Fay, L. Finco, S. Gascon, M. Gouzevitch, G. Grenier, B. Ille, F. Lagarde, I. B. Laktineh, H. Lattaud, M. Lethuillier, L. Mirabito, S. Perries, A. Popov[14], V. Sordini, G. Touquet, M. Vander Donckt, S. Viret

Georgian Technical University, Tbilisi, Georgia
A. Khvedelidze[8]

Tbilisi State University, Tbilisi, Georgia
Z. Tsamalaidze[8]

RWTH Aachen University, I. Physikalisches Institut, Aachen, Germany
C. Autermann, L. Feld, M. K. Kiesel, K. Klein, M. Lipinski, M. Preuten, M. P. Rauch, C. Schomakers, J. Schulz, M. Teroerde, B. Wittmer

RWTH Aachen University, III. Physikalisches Institut A, Aachen, Germany
A. Albert, D. Duchardt, M. Erdmann, S. Erdweg, T. Esch, R. Fischer, S. Ghosh, A. Güth, T. Hebbeker, C. Heidemann,
K. Hoepfner, H. Keller, L. Mastrolorenzo, M. Merschmeyer, A. Meyer, P. Millet, S. Mukherjee, T. Pook, M. Radziej,
H. Reithler, M. Rieger, A. Schmidt, D. Teyssier, S. Thüer

RWTH Aachen University, III. Physikalisches Institut B, Aachen, Germany
G. Flügge, O. Hlushchenko, T. Kress, A. Künsken, T. Müller, A. Nehrkorn, A. Nowack, C. Pistone, O. Pooth, D. Roy,
H. Sert, A. Stahl[15]

Deutsches Elektronen-Synchrotron, Hamburg, Germany
M. Aldaya Martin, T. Arndt, C. Asawatangtrakuldee, I. Babounikau, K. Beernaert, O. Behnke, U. Behrens,
A. Bermúdez Martínez, D. Bertsche, A. A. Bin Anuar, K. Borras[16], V. Botta, A. Campbell, P. Connor,
C. Contreras-Campana, V. Danilov, A. De Wit, M. M. Defranchis, C. Diez Pardos, D. Domínguez Damiani, G. Eckerlin,
T. Eichhorn, A. Elwood, E. Eren, E. Gallo[17], A. Geiser, A. Grohsjean, M. Guthoff, M. Haranko, A. Harb, J. Hauk, H. Jung,
M. Kasemann, J. Keaveney, C. Kleinwort, J. Knolle, D. Krücker, W. Lange, A. Lelek, T. Lenz, J. Leonard, K. Lipka,
W. Lohmann[18], R. Mankel, I.-A. Melzer-Pellmann, A. B. Meyer, M. Meyer, M. Missiroli, G. Mittag, J. Mnich,
V. Myronenko, S. K. Pflitsch, D. Pitzl, A. Raspereza, M. Savitskyi, P. Saxena, P. Schütze, C. Schwanenberger,
R. Shevchenko, A. Singh, H. Tholen, O. Turkot, A. Vagnerini, G. P. Van Onsem, R. Walsh, Y. Wen, K. Wichmann,
C. Wissing, O. Zenaiev

University of Hamburg, Hamburg, Germany
R. Aggleton, S. Bein, L. Benato, A. Benecke, V. Blobel, T. Dreyer, A. Ebrahimi, E. Garutti, D. Gonzalez, P. Gunnellini,
J. Haller, A. Hinzmann, A. Karavdina, G. Kasieczka, R. Klanner, R. Kogler, N. Kovalchuk, S. Kurz, V. Kutzner, J. Lange,
D. Marconi, J. Multhaup, M. Niedziela, C. E. N. Niemeyer, D. Nowatschin, A. Perieanu, A. Reimers, O. Rieger, C. Scharf,
P. Schleper, S. Schumann, J. Schwandt, J. Sonneveld, H. Stadie, G. Steinbrück, F. M. Stober, M. Stöver, A. Vanhoefer,
B. Vormwald, I. Zoi

Karlsruher Institut fuer Technologie, Karlsruhe, Germany
M. Akbiyik, C. Barth, M. Baselga, S. Baur, E. Butz, R. Caspart, T. Chwalek, F. Colombo, W. De Boer, A. Dierlamm,
K. El Morabit, N. Faltermann, B. Freund, M. Giffels, M. A. Harrendorf, F. Hartmann[15], S. M. Heindl, U. Husemann,
F. Kassel[15], I. Katkov[14], S. Kudella, S. Mitra, M. U. Mozer, Th. Müller, M. Plagge, G. Quast, K. Rabbertz, M. Schröder,
I. Shvetsov, G. Sieber, H. J. Simonis, R. Ulrich, S. Wayand, M. Weber, T. Weiler, S. Williamson, C. Wöhrmann, R. Wolf

Institute of Nuclear and Particle Physics (INPP), NCSR Demokritos, Aghia Paraskevi, Greece
G. Anagnostou, G. Daskalakis, T. Geralis, A. Kyriakis, D. Loukas, G. Paspalaki, I. Topsis-Giotis

National and Kapodistrian University of Athens, Athens, Greece
G. Karathanasis, S. Kesisoglou, P. Kontaxakis, A. Panagiotou, I. Papavergou, N. Saoulidou, E. Tziaferi, K. Vellidis

National Technical University of Athens, Athens, Greece
K. Kousouris, I. Papakrivopoulos, G. Tsipolitis

University of Ioánnina, Ioannina, Greece
I. Evangelou, C. Foudas, P. Gianneios, P. Katsoulis, P. Kokkas, S. Mallios, N. Manthos, I. Papadopoulos, E. Paradas,
J. Strologas, F. A. Triantis, D. Tsitsonis

MTA-ELTE Lendület CMS Particle and Nuclear Physics Group, Eötvös Loránd University, Budapest, Hungary
M. Bartók[19], M. Csanad, N. Filipovic, P. Major, M. I. Nagy, G. Pasztor, O. Surányi, G. I. Veres

Wigner Research Centre for Physics, Budapest, Hungary
G. Bencze, C. Hajdu, D. Horvath[20], Á. Hunyadi, F. Sikler, T. Á. Vámi, V. Veszpremi, G. Vesztergombi[†]

Institute of Nuclear Research ATOMKI, Debrecen, Hungary
N. Beni, S. Czellar, J. Karancsi[21], A. Makovec, J. Molnar, Z. Szillasi

Institute of Physics, University of Debrecen, Debrecen, Hungary
P. Raics, Z. L. Trocsanyi, B. Ujvari

Indian Institute of Science (IISc), Bangalore, India

S. Choudhury, J. R. Komaragiri, P. C. Tiwari

National Institute of Science Education and Research, HBNI, Bhubaneswar, India

S. Bahinipati[22], C. Kar, P. Mal, K. Mandal, A. Nayak[23], D. K. Sahoo[22], S. K. Swain

Panjab University, Chandigarh, India

S. Bansal, S. B. Beri, V. Bhatnagar, S. Chauhan, R. Chawla, N. Dhingra, R. Gupta, A. Kaur, M. Kaur, S. Kaur, R. Kumar, P. Kumari, M. Lohan, A. Mehta, K. Sandeep, S. Sharma, J. B. Singh, A. K. Virdi, G. Walia

University of Delhi, Delhi, India

A. Bhardwaj, B. C. Choudhary, R. B. Garg, M. Gola, S. Keshri, Ashok Kumar, S. Malhotra, M. Naimuddin, P. Priyanka, K. Ranjan, Aashaq Shah, R. Sharma

Saha Institute of Nuclear Physics, HBNI, Kolkata, India

R. Bhardwaj[24], M. Bharti[24], R. Bhattacharya, S. Bhattacharya, U. Bhawandeep[24], D. Bhowmik, S. Dey, S. Dutt[24], S. Dutta, S. Ghosh, K. Mondal, S. Nandan, A. Purohit, P. K. Rout, A. Roy, S. Roy Chowdhury, G. Saha, S. Sarkar, M. Sharan, B. Singh[24], S. Thakur[24]

Indian Institute of Technology Madras, Madras, India

P. K. Behera

Bhabha Atomic Research Centre, Mumbai, India

R. Chudasama, D. Dutta, V. Jha, V. Kumar, P. K. Netrakanti, L. M. Pant, P. Shukla

Tata Institute of Fundamental Research-A, Mumbai, India

T. Aziz, M. A. Bhat, S. Dugad, G. B. Mohanty, N. Sur, B. Sutar, RavindraKumar Verma

Tata Institute of Fundamental Research-B, Mumbai, India

S. Banerjee, S. Bhattacharya, S. Chatterjee, P. Das, M. Guchait, Sa. Jain, S. Karmakar, S. Kumar, M. Maity[25], G. Majumder, K. Mazumdar, N. Sahoo, T. Sarkar[25]

Indian Institute of Science Education and Research (IISER), Pune, India

S. Chauhan, S. Dube, V. Hegde, A. Kapoor, K. Kothekar, S. Pandey, A. Rane, S. Sharma

Institute for Research in Fundamental Sciences (IPM), Tehran, Iran

S. Chenarani[26], E. Eskandari Tadavani, S. M. Etesami[26], M. Khakzad, M. Mohammadi Najafabadi, M. Naseri, F. Rezaei Hosseinabadi, B. Safarzadeh[27], M. Zeinali

University College Dublin, Dublin, Ireland

M. Felcini, M. Grunewald

INFN Sezione di Bari[a], Università di Bari[b], Politecnico di Bari[c], Bari, Italy

M. Abbrescia[a,b], C. Calabria[a,b], A. Colaleo[a], D. Creanza[a,c], L. Cristella[a,b], N. De Filippis[a,c], M. De Palma[a,b], A. Di Florio[a,b], F. Errico[a,b], L. Fiore[a], A. Gelmi[a,b], G. Iaselli[a,c], M. Ince[a,b], S. Lezki[a,b], G. Maggi[a,c], M. Maggi[a], G. Miniello[a,b], S. My[a,b], S. Nuzzo[a,b], A. Pompili[a,b], G. Pugliese[a,c], R. Radogna[a], A. Ranieri[a], G. Selvaggi[a,b], A. Sharma[a], L. Silvestris[a], R. Venditti[a], P. Verwilligen[a], G. Zito[a]

INFN Sezione di Bologna[a], Università di Bologna[b], Bologna, Italy

G. Abbiendi[a], C. Battilana[a,b], D. Bonacorsi[a,b], L. Borgonovi[a,b], S. Braibant-Giacomelli[a,b], R. Campanini[a,b], P. Capiluppi[a,b], A. Castro[a,b], F. R. Cavallo[a], S. S. Chhibra[a,b], C. Ciocca[a], G. Codispoti[a,b], M. Cuffiani[a,b], G. M. Dallavalle[a], F. Fabbri[a], A. Fanfani[a,b], E. Fontanesi, P. Giacomelli[a], C. Grandi[a], L. Guiducci[a,b], F. Iemmi[a,b], S. Lo Meo[a], S. Marcellini[a], G. Masetti[a], A. Montanari[a], F. L. Navarria[a,b], A. Perrotta[a], F. Primavera[a,b,15], T. Rovelli[a,b], G. P. Siroli[a,b], N. Tosi[a]

INFN Sezione di Catania[a], Università di Catania[b], Catania, Italy

S. Albergo[a,b], A. Di Mattia[a], R. Potenza[a,b], A. Tricomi[a,b], C. Tuve[a,b]

INFN Sezione di Firenze[a], Università di Firenze[b], Firenze, Italy

G. Barbagli[a], K. Chatterjee[a,b], V. Ciulli[a,b], C. Civinini[a], R. D'Alessandro[a,b], E. Focardi[a,b], G. Latino, P. Lenzi[a,b], M. Meschini[a], S. Paoletti[a], L. Russo[a,28], G. Sguazzoni[a], D. Strom[a], L. Viliani[a]

INFN Laboratori Nazionali di Frascati, Frascati, Italy

L. Benussi, S. Bianco, F. Fabbri, D. Piccolo

INFN Sezione di Genova[a], Università di Genova[b], Genova, Italy

F. Ferro[a], F. Ravera[a,b], E. Robutti[a], S. Tosi[a,b]

INFN Sezione di Milano-Bicocca[a], Università di Milano-Bicocca[b], Milan, Italy

A. Benaglia[a], A. Beschi[b], F. Brivio[a,b], V. Ciriolo[a,b,15], S. Di Guida[a,d,15], M. E. Dinardo[a,b], S. Fiorendi[a,b], S. Gennai[a], A. Ghezzi[a,b], P. Govoni[a,b], M. Malberti[a,b], S. Malvezzi[a], A. Massironi[a,b], D. Menasce[a], F. Monti, L. Moroni[a], M. Paganoni[a,b], D. Pedrini[a], S. Ragazzi[a,b], T. Tabarelli de Fatis[a,b], D. Zuolo[a,b]

INFN Sezione di Napoli[a], Università di Napoli 'Federico II'[b], Napoli, Italy, Università della Basilicata[c], Potenza, Italy, Università G. Marconi[d], Rome, Italy

S. Buontempo[a], N. Cavallo[a,c], A. De Iorio[a,b], A. Di Crescenzo[a,b], F. Fabozzi[a,c], F. Fienga[a], G. Galati[a], A. O. M. Iorio[a,b], W. A. Khan[a], L. Lista[a], S. Meola[a,d,15], P. Paolucci[a,15], C. Sciacca[a,b], E. Voevodina[a,b]

INFN Sezione di Padova[a], Università di Padova[b], Padova, Italy, Università di Trento[c], Trento, Italy

P. Azzi[a], N. Bacchetta[a], D. Bisello[a,b], A. Boletti[a,b], A. Bragagnolo, R. Carlin[a,b], P. Checchia[a], M. Dall'Osso[a,b], P. De Castro Manzano[a], T. Dorigo[a], U. Dosselli[a], F. Gasparini[a,b], U. Gasparini[a,b], A. Gozzelino[a], S. Y. Hoh, S. Lacaprara[a], P. Lujan, M. Margoni[a,b], A. T. Meneguzzo[a,b], J. Pazzini[a,b], P. Ronchese[a,b], R. Rossin[a,b], F. Simonetto[a,b], A. Tiko, E. Torassa[a], M. Zanetti[a,b], P. Zotto[a,b], G. Zumerle[a,b]

INFN Sezione di Pavia[a], Università di Pavia[b], Pavia, Italy

A. Braghieri[a], A. Magnani[a], P. Montagna[a,b], S. P. Ratti[a,b], V. Re[a], M. Ressegotti[a,b], C. Riccardi[a,b], P. Salvini[a], I. Vai[a,b], P. Vitulo[a,b]

INFN Sezione di Perugia[a], Università di Perugia[b], Perugia, Italy

M. Biasini[a,b], G. M. Bilei[a], C. Cecchi[a,b], D. Ciangottini[a,b], L. Fanò[a,b], P. Lariccia[a,b], R. Leonardi[a,b], E. Manoni[a], G. Mantovani[a,b], V. Mariani[a,b], M. Menichelli[a], A. Rossi[a,b], A. Santocchia[a,b], D. Spiga[a]

INFN Sezione di Pisa[a], Università di Pisa[b], Scuola Normale Superiore di Pisa[c], Pisa, Italy

K. Androsov[a], P. Azzurri[a], G. Bagliesi[a], L. Bianchini[a], T. Boccali[a], L. Borrello, R. Castaldi[a], M. A. Ciocci[a,b], R. Dell'Orso[a], G. Fedi[a], F. Fiori[a,c], L. Giannini[a,c], A. Giassi[a], M. T. Grippo[a], F. Ligabue[a,c], E. Manca[a,c], G. Mandorli[a,c], A. Messineo[a,b], F. Palla[a], A. Rizzi[a,b], G. Rolandi[29], P. Spagnolo[a], R. Tenchini[a], G. Tonelli[a,b], A. Venturi[a], P. G. Verdini[a]

INFN Sezione di Roma[a], Sapienza Università di Roma[b], Rome, Italy

L. Barone[a,b], F. Cavallari[a], M. Cipriani[a,b], D. Del Re[a,b], E. Di Marco[a,b], M. Diemoz[a], S. Gelli[a,b], E. Longo[a,b], B. Marzocchi[a,b], P. Meridiani[a], G. Organtini[a,b], F. Pandolfi[a], R. Paramatti[a,b], F. Preiato[a,b], S. Rahatlou[a,b], C. Rovelli[a], F. Santanastasio[a,b]

INFN Sezione di Torino[a], Università di Torino[b], Torino, Italy, Università del Piemonte Orientale[c], Novara, Italy

N. Amapane[a,b], R. Arcidiacono[a,c], S. Argiro[a,b], M. Arneodo[a,c], N. Bartosik[a], R. Bellan[a,b], C. Biino[a], N. Cartiglia[a], F. Cenna[a,b], S. Cometti[a], M. Costa[a,b], R. Covarelli[a,b], N. Demaria[a], B. Kiani[a,b], C. Mariotti[a], S. Maselli[a], E. Migliore[a,b], V. Monaco[a,b], E. Monteil[a,b], M. Monteno[a], M. M. Obertino[a,b], L. Pacher[a,b], N. Pastrone[a], M. Pelliccioni[a], G. L. Pinna Angioni[a,b], A. Romero[a,b], M. Ruspa[a,c], R. Sacchi[a,b], K. Shchelina[a,b], V. Sola[a], A. Solano[a,b], D. Soldi[a,b], A. Staiano[a]

INFN Sezione di Trieste[a], Università di Trieste[b], Trieste, Italy

S. Belforte[a], V. Candelise[a,b], M. Casarsa[a], F. Cossutti[a], A. Da Rold[a,b], G. Della Ricca[a,b], F. Vazzoler[a,b], A. Zanetti[a]

Kyungpook National University, Daegu, Korea

D. H. Kim, G. N. Kim, M. S. Kim, J. Lee, S. Lee, S. W. Lee, C. S. Moon, Y. D. Oh, S. I. Pak, S. Sekmen, D. C. Son, Y. C. Yang

Chonnam National University, Institute for Universe and Elementary Particles, Kwangju, Korea
H. Kim, D. H. Moon, G. Oh

Hanyang University, Seoul, Korea
B. Francois, J. Goh[30], T. J. Kim

Korea University, Seoul, Korea
S. Cho, S. Choi, Y. Go, D. Gyun, S. Ha, B. Hong, Y. Jo, K. Lee, K. S. Lee, S. Lee, J. Lim, S. K. Park, Y. Roh

Sejong University, Seoul, Korea
H. S. Kim

Seoul National University, Seoul, Korea
J. Almond, J. Kim, J. S. Kim, H. Lee, K. Lee, K. Nam, S. B. Oh, B. C. Radburn-Smith, S. h. Seo, U. K. Yang, H. D. Yoo, G. B. Yu

University of Seoul, Seoul, Korea
D. Jeon, H. Kim, J. H. Kim, J. S. H. Lee, I. C. Park

Sungkyunkwan University, Suwon, Korea
Y. Choi, C. Hwang, J. Lee, I. Yu

Vilnius University, Vilnius, Lithuania
V. Dudenas, A. Juodagalvis, J. Vaitkus

National Centre for Particle Physics, Universiti Malaya, Kuala Lumpur, Malaysia
I. Ahmed, Z. A. Ibrahim, M. A. B. Md Ali[31], F. Mohamad Idris[32], W. A. T. Wan Abdullah, M. N. Yusli, Z. Zolkapli

Universidad de Sonora (UNISON), Hermosillo, Mexico
J. F. Benitez, A. Castaneda Hernandez, J. A. Murillo Quijada

Centro de Investigacion y de Estudios Avanzados del IPN, Mexico City, Mexico
H. Castilla-Valdez, E. De La Cruz-Burelo, M. C. Duran-Osuna, I. Heredia-De La Cruz[33], R. Lopez-Fernandez, J. Mejia Guisao, R. I. Rabadan-Trejo, M. Ramirez-Garcia, G. Ramirez-Sanchez, R. Reyes-Almanza, A. Sanchez-Hernandez

Universidad Iberoamericana, Mexico City, Mexico
S. Carrillo Moreno, C. Oropeza Barrera, F. Vazquez Valencia

Benemerita Universidad Autonoma de Puebla, Puebla, Mexico
J. Eysermans, I. Pedraza, H. A. Salazar Ibarguen, C. Uribe Estrada

Universidad Autónoma de San Luis Potosí, San Luis Potosí, Mexico
A. Morelos Pineda

University of Auckland, Auckland, New Zealand
D. Krofcheck

University of Canterbury, Christchurch, New Zealand
S. Bheesette, P. H. Butler

National Centre for Physics, Quaid-I-Azam University, Islamabad, Pakistan
A. Ahmad, M. Ahmad, M. I. Asghar, Q. Hassan, H. R. Hoorani, A. Saddique, M. A. Shah, M. Shoaib, M. Waqas

National Centre for Nuclear Research, Swierk, Poland
H. Bialkowska, M. Bluj, B. Boimska, T. Frueboes, M. Górski, M. Kazana, M. Szleper, P. Traczyk, P. Zalewski

Institute of Experimental Physics, Faculty of Physics, University of Warsaw, Warsaw, Poland
K. Bunkowski, A. Byszuk[34], K. Doroba, A. Kalinowski, M. Konecki, J. Krolikowski, M. Misiura, M. Olszewski, A. Pyskir, M. Walczak

Laboratório de Instrumentação e Física Experimental de Partículas, Lisboa, Portugal
M. Araujo, P. Bargassa, C. Beirão Da Cruz E Silva, A. Di Francesco, P. Faccioli, B. Galinhas, M. Gallinaro, J. Hollar, N. Leonardo, M. V. Nemallapudi, J. Seixas, G. Strong, O. Toldaiev, D. Vadruccio, J. Varela

Joint Institute for Nuclear Research, Dubna, Russia
S. Afanasiev, P. Bunin, M. Gavrilenko, I. Golutvin, I. Gorbunov, A. Kamenev, V. Karjavine, A. Lanev, A. Malakhov,
V. Matveev[35,36], P. Moisenz, V. Palichik, V. Perelygin, S. Shmatov, S. Shulha, N. Skatchkov, V. Smirnov, N. Voytishin,
A. Zarubin

Petersburg Nuclear Physics Institute, Gatchina (St. Petersburg), Russia
V. Golovtsov, Y. Ivanov, V. Kim[37], E. Kuznetsova[38], P. Levchenko, V. Murzin, V. Oreshkin, I. Smirnov, D. Sosnov,
V. Sulimov, L. Uvarov, S. Vavilov, A. Vorobyev

Institute for Nuclear Research, Moscow, Russia
Yu. Andreev, A. Dermenev, S. Gninenko, N. Golubev, A. Karneyeu, M. Kirsanov, N. Krasnikov, A. Pashenkov, D. Tlisov,
A. Toropin

Institute for Theoretical and Experimental Physics, Moscow, Russia
V. Epshteyn, V. Gavrilov, N. Lychkovskaya, V. Popov, I. Pozdnyakov, G. Safronov, A. Spiridonov, A. Stepennov,
V. Stolin, M. Toms, E. Vlasov, A. Zhokin

Moscow Institute of Physics and Technology, Moscow, Russia
T. Aushev

National Research Nuclear University 'Moscow Engineering Physics Institute' (MEPhI), Moscow, Russia
M. Chadeeva[39], P. Parygin, D. Philippov, S. Polikarpov[39], E. Popova, V. Rusinov

P.N. Lebedev Physical Institute, Moscow, Russia
V. Andreev, M. Azarkin, I. Dremin[36], M. Kirakosyan, S. V. Rusakov, A. Terkulov

Skobeltsyn Institute of Nuclear Physics, Lomonosov Moscow State University, Moscow, Russia
A. Baskakov, A. Belyaev, E. Boos, M. Dubinin[40], L. Dudko, A. Ershov, A. Gribushin, V. Klyukhin, O. Kodolova,
I. Lokhtin, I. Miagkov, S. Obraztsov, S. Petrushanko, V. Savrin, A. Snigirev

Novosibirsk State University (NSU), Novosibirsk, Russia
A. Barnyakov[41], V. Blinov[41], T. Dimova[41], L. Kardapoltsev[41], Y. Skovpen[41]

Institute for High Energy Physics of National Research Centre 'Kurchatov Institute', Protvino, Russia
I. Azhgirey, I. Bayshev, S. Bitioukov, D. Elumakhov, A. Godizov, V. Kachanov, A. Kalinin, D. Konstantinov, P. Mandrik,
V. Petrov, R. Ryutin, S. Slabospitskii, A. Sobol, S. Troshin, N. Tyurin, A. Uzunian, A. Volkov

National Research Tomsk Polytechnic University, Tomsk, Russia
A. Babaev, S. Baidali, V. Okhotnikov

University of Belgrade, Faculty of Physics and Vinca Institute of Nuclear Sciences, Belgrade, Serbia
P. Adzic[42], P. Cirkovic, D. Devetak, M. Dordevic, J. Milosevic

Centro de Investigaciones Energéticas Medioambientales y Tecnológicas (CIEMAT), Madrid, Spain
J. Alcaraz Maestre, A. Álvarez Fernández, I. Bachiller, M. Barrio Luna, J. A. Brochero Cifuentes, M. Cerrada, N. Colino,
B. De La Cruz, A. Delgado Peris, C. Fernandez Bedoya, J. P. Fernández Ramos, J. Flix, M. C. Fouz, O. Gonzalez Lopez,
S. Goy Lopez, J. M. Hernandez, M. I. Josa, D. Moran, A. Pérez-Calero Yzquierdo, J. Puerta Pelayo, I. Redondo,
L. Romero, M. S. Soares, A. Triossi

Universidad Autónoma de Madrid, Madrid, Spain
C. Albajar, J. F. de Trocóniz

Universidad de Oviedo, Oviedo, Spain
J. Cuevas, C. Erice, J. Fernandez Menendez, S. Folgueras, I. Gonzalez Caballero, J. R. González Fernández,
E. Palencia Cortezon, V. Rodríguez Bouza, S. Sanchez Cruz, P. Vischia, J. M. Vizan Garcia

Instituto de Física de Cantabria (IFCA), CSIC-Universidad de Cantabria, Santander, Spain

I. J. Cabrillo, A. Calderon, B. Chazin Quero, J. Duarte Campderros, M. Fernandez, P. J. Fernández Manteca, A. García Alonso, J. Garcia-Ferrero, G. Gomez, A. Lopez Virto, J. Marco, C. Martinez Rivero, P. Martinez Ruiz del Arbol, F. Matorras, J. Piedra Gomez, C. Prieels, T. Rodrigo, A. Ruiz-Jimeno, L. Scodellaro, N. Trevisani, I. Vila, R. Vilar Cortabitarte

Department of Physics, University of Ruhuna, Matara, Sri Lanka

N. Wickramage

CERN, European Organization for Nuclear Research, Geneva, Switzerland

D. Abbaneo, B. Akgun, E. Auffray, G. Auzinger, P. Baillon, A. H. Ball, D. Barney, J. Bendavid, M. Bianco, A. Bocci, C. Botta, E. Brondolin, T. Camporesi, M. Cepeda, G. Cerminara, E. Chapon, Y. Chen, G. Cucciati, D. d'Enterria, A. Dabrowski, N. Daci, V. Daponte, A. David, A. De Roeck, N. Deelen, M. Dobson, M. Dünser, N. Dupont, A. Elliott-Peisert, P. Everaerts, F. Fallavollita[43], D. Fasanella, G. Franzoni, J. Fulcher, W. Funk, D. Gigi, A. Gilbert, K. Gill, F. Glege, M. Guilbaud, D. Gulhan, J. Hegeman, C. Heidegger, V. Innocente, A. Jafari, P. Janot, O. Karacheban[18], J. Kieseler, A. Kornmayer, M. Krammer[1], C. Lange, P. Lecoq, C. Lourenço, L. Malgeri, M. Mannelli, F. Meijers, J. A. Merlin, S. Mersi, E. Meschi, P. Milenovic[44], F. Moortgat, M. Mulders, J. Ngadiuba, S. Nourbakhsh, S. Orfanelli, L. Orsini, F. Pantaleo[15], L. Pape, E. Perez, M. Peruzzi, A. Petrilli, G. Petrucciani, A. Pfeiffer, M. Pierini, F. M. Pitters, D. Rabady, A. Racz, T. Reis, M. Rovere, H. Sakulin, C. Schäfer, C. Schwick, M. Seidel, M. Selvaggi, A. Sharma, P. Silva, P. Sphicas[45], A. Stakia, J. Steggemann, M. Tosi, D. Treille, A. Tsirou, V. Veckalns[46], M. Verzetti, W. D. Zeuner

Paul Scherrer Institut, Villigen, Switzerland

L. Caminada[47], K. Deiters, W. Erdmann, R. Horisberger, Q. Ingram, H. C. Kaestli, D. Kotlinski, U. Langenegger, T. Rohe, S. A. Wiederkehr

ETH Zurich - Institute for Particle Physics and Astrophysics (IPA), Zurich, Switzerland

M. Backhaus, L. Bäni, P. Berger, N. Chernyavskaya, G. Dissertori, M. Dittmar, M. Donegà, C. Dorfer, T. A. Gómez Espinosa, C. Grab, D. Hits, T. Klijnsma, W. Lustermann, R. A. Manzoni, M. Marionneau, M. T. Meinhard, F. Micheli, P. Musella, F. Nessi-Tedaldi, J. Pata, F. Pauss, G. Perrin, L. Perrozzi, S. Pigazzini, M. Quittnat, C. Reissel, D. Ruini, D. A. Sanz Becerra, M. Schönenberger, L. Shchutska, V. R. Tavolaro, K. Theofilatos, M. L. Vesterbacka Olsson, R. Wallny, D. H. Zhu

Universität Zürich, Zurich, Switzerland

T. K. Aarrestad, C. Amsler[48], D. Brzhechko, M. F. Canelli, A. De Cosa, R. Del Burgo, S. Donato, C. Galloni, T. Hreus, B. Kilminster, S. Leontsinis, I. Neutelings, G. Rauco, P. Robmann, D. Salerno, K. Schweiger, C. Seitz, Y. Takahashi, A. Zucchetta

National Central University, Chung-Li, Taiwan

Y. H. Chang, K. y. Cheng, T. H. Doan, H. R. Jheng, R. Khurana, C. M. Kuo, W. Lin, A. Pozdnyakov, S. S. Yu

National Taiwan University (NTU), Taipei, Taiwan

P. Chang, Y. Chao, K. F. Chen, P. H. Chen, W.-S. Hou, Arun Kumar, Y. F. Liu, R.-S. Lu, E. Paganis, A. Psallidas, A. Steen

Chulalongkorn University, Faculty of Science, Department of Physics, Bangkok, Thailand

B. Asavapibhop, N. Srimanobhas, N. Suwonjandee

Çukurova University, Physics Department, Science and Art Faculty, Adana, Turkey

M. N. Bakirci[49], A. Bat, F. Boran, S. Cerci[50], S. Damarseckin, Z. S. Demiroglu, F. Dolek, C. Dozen, I. Dumanoglu, E. Eskut, S. Girgis, G. Gokbulut, Y. Guler, E. Gurpinar, I. Hos[51], C. Isik, E. E. Kangal[52], O. Kara, A. Kayis Topaksu, U. Kiminsu, M. Oglakci, G. Onengut, K. Ozdemir[53], A. Polatoz, U. G. Tok, S. Turkcapar, I. S. Zorbakir, C. Zorbilmez

Middle East Technical University, Physics Department, Ankara, Turkey

B. Isildak[54], G. Karapinar[55], M. Yalvac, M. Zeyrek

Bogazici University, Istanbul, Turkey

I. O. Atakisi, E. Gülmez, M. Kaya[56], O. Kaya[57], S. Ozkorucuklu[58], S. Tekten, E. A. Yetkin[59]

Istanbul Technical University, Istanbul, Turkey

M. N. Agaras, A. Cakir, K. Cankocak, Y. Komurcu, S. Sen[60]

Institute for Scintillation Materials of National Academy of Science of Ukraine, Kharkov, Ukraine
B. Grynyov

National Scientific Center, Kharkov Institute of Physics and Technology, Kharkov, Ukraine
L. Levchuk

University of Bristol, Bristol, United Kingdom
F. Ball, L. Beck, J. J. Brooke, D. Burns, E. Clement, D. Cussans, O. Davignon, H. Flacher, J. Goldstein, G. P. Heath, H. F. Heath, L. Kreczko, D. M. Newbold[61], S. Paramesvaran, B. Penning, T. Sakuma, D. Smith, V. J. Smith, J. Taylor, A. Titterton

Rutherford Appleton Laboratory, Didcot, United Kingdom
K. W. Bell, A. Belyaev[62], C. Brew, R. M. Brown, D. Cieri, D. J. A. Cockerill, J. A. Coughlan, K. Harder, S. Harper, J. Linacre, E. Olaiya, D. Petyt, C. H. Shepherd-Themistocleous, A. Thea, I. R. Tomalin, T. Williams, W. J. Womersley

Imperial College, London, United Kingdom
R. Bainbridge, P. Bloch, J. Borg, S. Breeze, O. Buchmuller, A. Bundock, D. Colling, P. Dauncey, G. Davies, M. Della Negra, R. Di Maria, G. Hall, G. Iles, T. James, M. Komm, C. Laner, L. Lyons, A.-M. Magnan, S. Malik, A. Martelli, J. Nash[63], A. Nikitenko[7], V. Palladino, M. Pesaresi, D. M. Raymond, A. Richards, A. Rose, E. Scott, C. Seez, A. Shtipliyski, G. Singh, M. Stoye, T. Strebler, S. Summers, A. Tapper, K. Uchida, T. Virdee[15], N. Wardle, D. Winterbottom, J. Wright, S. C. Zenz

Brunel University, Uxbridge, United Kingdom
J. E. Cole, P. R. Hobson, A. Khan, P. Kyberd, C. K. Mackay, A. Morton, I. D. Reid, L. Teodorescu, S. Zahid

Baylor University, Waco, USA
K. Call, J. Dittmann, K. Hatakeyama, H. Liu, C. Madrid, B. Mcmaster, N. Pastika, C. Smith

Catholic University of America, Washington DC, USA
R. Bartek, A. Dominguez

The University of Alabama, Tuscaloosa, USA
A. Buccilli, S. I. Cooper, C. Henderson, P. Rumerio, C. West

Boston University, Boston, USA
D. Arcaro, T. Bose, D. Gastler, D. Pinna, D. Rankin, C. Richardson, J. Rohlf, L. Sulak, D. Zou

Brown University, Providence, USA
G. Benelli, X. Coubez, D. Cutts, M. Hadley, J. Hakala, U. Heintz, J. M. Hogan[64], K. H. M. Kwok, E. Laird, G. Landsberg, J. Lee, Z. Mao, M. Narain, S. Sagir[65], R. Syarif, E. Usai, D. Yu

University of California, Davis, Davis, USA
R. Band, C. Brainerd, R. Breedon, D. Burns, M. Calderon De La Barca Sanchez, M. Chertok, J. Conway, R. Conway, P. T. Cox, R. Erbacher, C. Flores, G. Funk, W. Ko, O. Kukral, R. Lander, M. Mulhearn, D. Pellett, J. Pilot, S. Shalhout, M. Shi, D. Stolp, D. Taylor, K. Tos, M. Tripathi, Z. Wang, F. Zhang

University of California, Los Angeles, USA
M. Bachtis, C. Bravo, R. Cousins, A. Dasgupta, A. Florent, J. Hauser, M. Ignatenko, N. Mccoll, S. Regnard, D. Saltzberg, C. Schnaible, V. Valuev

University of California, Riverside, Riverside, USA
E. Bouvier, K. Burt, R. Clare, J. W. Gary, S. M. A. Ghiasi Shirazi, G. Hanson, G. Karapostoli, E. Kennedy, F. Lacroix, O. R. Long, M. Olmedo Negrete, M. I. Paneva, W. Si, L. Wang, H. Wei, S. Wimpenny, B. R. Yates

University of California, San Diego, La Jolla, USA
J. G. Branson, P. Chang, S. Cittolin, M. Derdzinski, R. Gerosa, D. Gilbert, B. Hashemi, A. Holzner, D. Klein, G. Kole, V. Krutelyov, J. Letts, M. Masciovecchio, D. Olivito, S. Padhi, M. Pieri, M. Sani, V. Sharma, S. Simon, M. Tadel, A. Vartak, S. Wasserbaech[66], J. Wood, F. Würthwein, A. Yagil, G. Zevi Della Porta

University of California, Santa Barbara - Department of Physics, Santa Barbara, USA

N. Amin, R. Bhandari, J. Bradmiller-Feld, C. Campagnari, M. Citron, A. Dishaw, V. Dutta, M. Franco Sevilla, L. Gouskos, R. Heller, J. Incandela, A. Ovcharova, H. Qu, J. Richman, D. Stuart, I. Suarez, S. Wang, J. Yoo

California Institute of Technology, Pasadena, USA

D. Anderson, A. Bornheim, J. M. Lawhorn, H. B. Newman, T. Q. Nguyen, M. Spiropulu, J. R. Vlimant, R. Wilkinson, S. Xie, Z. Zhang, R. Y. Zhu

Carnegie Mellon University, Pittsburgh, USA

M. B. Andrews, T. Ferguson, T. Mudholkar, M. Paulini, M. Sun, I. Vorobiev, M. Weinberg

University of Colorado Boulder, Boulder, USA

J. P. Cumalat, W. T. Ford, F. Jensen, A. Johnson, M. Krohn, E. MacDonald, T. Mulholland, R. Patel, A. Perloff, K. Stenson, K. A. Ulmer, S. R. Wagner

Cornell University, Ithaca, USA

J. Alexander, J. Chaves, Y. Cheng, J. Chu, A. Datta, K. Mcdermott, N. Mirman, J. R. Patterson, D. Quach, A. Rinkevicius, A. Ryd, L. Skinnari, L. Soffi, S. M. Tan, Z. Tao, J. Thom, J. Tucker, P. Wittich, M. Zientek

Fermi National Accelerator Laboratory, Batavia, USA

S. Abdullin, M. Albrow, M. Alyari, G. Apollinari, A. Apresyan, A. Apyan, S. Banerjee, L. A. T. Bauerdick, A. Beretvas, J. Berryhill, P. C. Bhat, K. Burkett, J. N. Butler, A. Canepa, G. B. Cerati, H. W. K. Cheung, F. Chlebana, M. Cremonesi, J. Duarte, V. D. Elvira, J. Freeman, Z. Gecse, E. Gottschalk, L. Gray, D. Green, S. Grünendahl, O. Gutsche, J. Hanlon, R. M. Harris, S. Hasegawa, J. Hirschauer, Z. Hu, B. Jayatilaka, S. Jindariani, M. Johnson, U. Joshi, B. Klima, M. J. Kortelainen, B. Kreis, S. Lammel, D. Lincoln, R. Lipton, M. Liu, T. Liu, J. Lykken, K. Maeshima, J. M. Marraffino, D. Mason, P. McBride, P. Merkel, S. Mrenna, S. Nahn, V. O'Dell, K. Pedro, C. Pena, O. Prokofyev, G. Rakness, L. Ristori, A. Savoy-Navarro[67], B. Schneider, E. Sexton-Kennedy, A. Soha, W. J. Spalding, L. Spiegel, S. Stoynev, J. Strait, N. Strobbe, L. Taylor, S. Tkaczyk, N. V. Tran, L. Uplegger, E. W. Vaandering, C. Vernieri, M. Verzocchi, R. Vidal, M. Wang, H. A. Weber, A. Whitbeck

University of Florida, Gainesville, USA

D. Acosta, P. Avery, P. Bortignon, D. Bourilkov, A. Brinkerhoff, L. Cadamuro, A. Carnes, M. Carver, D. Curry, R. D. Field, S. V. Gleyzer, B. M. Joshi, J. Konigsberg, A. Korytov, K. H. Lo, P. Ma, K. Matchev, H. Mei, G. Mitselmakher, D. Rosenzweig, K. Shi, D. Sperka, J. Wang, S. Wang, X. Zuo

Florida International University, Miami, USA

Y. R. Joshi, S. Linn

Florida State University, Tallahassee, USA

A. Ackert, T. Adams, A. Askew, S. Hagopian, V. Hagopian, K. F. Johnson, T. Kolberg, G. Martinez, T. Perry, H. Prosper, A. Saha, C. Schiber, R. Yohay

Florida Institute of Technology, Melbourne, USA

M. M. Baarmand, V. Bhopatkar, S. Colafranceschi, M. Hohlmann, D. Noonan, M. Rahmani, T. Roy, F. Yumiceva

University of Illinois at Chicago (UIC), Chicago, USA

M. R. Adams, L. Apanasevich, D. Berry, R. R. Betts, R. Cavanaugh, X. Chen, S. Dittmer, O. Evdokimov, C. E. Gerber, D. A. Hangal, D. J. Hofman, K. Jung, J. Kamin, C. Mills, I. D. Sandoval Gonzalez, M. B. Tonjes, H. Trauger, N. Varelas, H. Wang, X. Wang, Z. Wu, J. Zhang

The University of Iowa, Iowa City, USA

M. Alhusseini, B. Bilki[68], W. Clarida, K. Dilsiz[69], S. Durgut, R. P. Gandrajula, M. Haytmyradov, V. Khristenko, J.-P. Merlo, A. Mestvirishvili, A. Moeller, J. Nachtman, H. Ogul[70], Y. Onel, F. Ozok[71], A. Penzo, C. Snyder, E. Tiras, J. Wetzel

Johns Hopkins University, Baltimore, USA

B. Blumenfeld, A. Cocoros, N. Eminizer, D. Fehling, L. Feng, A. V. Gritsan, W. T. Hung, P. Maksimovic, J. Roskes,
U. Sarica, M. Swartz, M. Xiao, C. You

The University of Kansas, Lawrence, USA

A. Al-bataineh, P. Baringer, A. Bean, S. Boren, J. Bowen, A. Bylinkin, J. Castle, S. Khalil, A. Kropivnitskaya,
D. Majumder, W. Mcbrayer, M. Murray, C. Rogan, S. Sanders, E. Schmitz, J. D. Tapia Takaki, Q. Wang

Kansas State University, Manhattan, USA

S. Duric, A. Ivanov, K. Kaadze, D. Kim, Y. Maravin, D. R. Mendis, T. Mitchell, A. Modak, A. Mohammadi, L. K. Saini,
N. Skhirtladze

Lawrence Livermore National Laboratory, Livermore, USA

F. Rebassoo, D. Wright

University of Maryland, College Park, USA

A. Baden, O. Baron, A. Belloni, S. C. Eno, Y. Feng, C. Ferraioli, N. J. Hadley, S. Jabeen, G. Y. Jeng, R. G. Kellogg,
J. Kunkle, A. C. Mignerey, S. Nabili, F. Ricci-Tam, Y. H. Shin, A. Skuja, S. C. Tonwar, K. Wong

Massachusetts Institute of Technology, Cambridge, USA

D. Abercrombie, B. Allen, V. Azzolini, A. Baty, G. Bauer, R. Bi, S. Brandt, W. Busza, I. A. Cali, M. D'Alfonso,
Z. Demiragli, G. Gomez Ceballos, M. Goncharov, P. Harris, D. Hsu, M. Hu, Y. Iiyama, G. M. Innocenti, M. Klute,
D. Kovalskyi, Y.-J. Lee, P. D. Luckey, B. Maier, A. C. Marini, C. Mcginn, C. Mironov, S. Narayanan, X. Niu, C. Paus,
C. Roland, G. Roland, G. S. F. Stephans, K. Sumorok, K. Tatar, D. Velicanu, J. Wang, T. W. Wang, B. Wyslouch,
S. Zhaozhong

University of Minnesota, Minneapolis, USA

A. C. Benvenuti[†], R. M. Chatterjee, A. Evans, P. Hansen, J. Hiltbrand, Sh. Jain, S. Kalafut, Y. Kubota, Z. Lesko, J. Mans,
N. Ruckstuhl, R. Rusack, M. A. Wadud

University of Mississippi, Oxford, USA

J. G. Acosta, S. Oliveros

University of Nebraska-Lincoln, Lincoln, USA

E. Avdeeva, K. Bloom, D. R. Claes, C. Fangmeier, F. Golf, R. Gonzalez Suarez, R. Kamalieddin, I. Kravchenko,
J. Monroy, J. E. Siado, G. R. Snow, B. Stieger

State University of New York at Buffalo, Buffalo, USA

A. Godshalk, C. Harrington, I. Iashvili, A. Kharchilava, C. Mclean, D. Nguyen, A. Parker, S. Rappoccio, B. Roozbahani

Northeastern University, Boston, USA

G. Alverson, E. Barberis, C. Freer, Y. Haddad, A. Hortiangtham, D. M. Morse, T. Orimoto, R. Teixeira De Lima,
T. Wamorkar, B. Wang, A. Wisecarver, D. Wood

Northwestern University, Evanston, USA

S. Bhattacharya, O. Charaf, K. A. Hahn, N. Mucia, N. Odell, M. H. Schmitt, K. Sung, M. Trovato, M. Velasco

University of Notre Dame, Notre Dame, USA

R. Bucci, N. Dev, M. Hildreth, K. Hurtado Anampa, C. Jessop, D. J. Karmgard, N. Kellams, K. Lannon, W. Li, N. Loukas,
N. Marinelli, F. Meng, C. Mueller, Y. Musienko[35], M. Planer, A. Reinsvold, R. Ruchti, P. Siddireddy, G. Smith, S. Taroni,
M. Wayne, A. Wightman, M. Wolf, A. Woodard

The Ohio State University, Columbus, USA

J. Alimena, L. Antonelli, B. Bylsma, L. S. Durkin, S. Flowers, B. Francis, A. Hart, C. Hill, W. Ji, T. Y. Ling, W. Luo,
B. L. Winer

Princeton University, Princeton, USA

S. Cooperstein, P. Elmer, J. Hardenbrook, S. Higginbotham, A. Kalogeropoulos, D. Lange, M. T. Lucchini, J. Luo,
D. Marlow, K. Mei, I. Ojalvo, J. Olsen, C. Palmer, P. Piroué, J. Salfeld-Nebgen, D. Stickland, C. Tully

University of Puerto Rico, Mayaguez, USA

S. Malik, S. Norberg

Purdue University, West Lafayette, USA

A. Barker, V. E. Barnes, S. Das, L. Gutay, M. Jones, A. W. Jung, A. Khatiwada, B. Mahakud, D. H. Miller, N. Neumeister, C. C. Peng, S. Piperov, H. Qiu, J. F. Schulte, J. Sun, F. Wang, R. Xiao, W. Xie

Purdue University Northwest, Hammond, USA

T. Cheng, J. Dolen, N. Parashar

Rice University, Houston, USA

Z. Chen, K. M. Ecklund, S. Freed, F. J. M. Geurts, M. Kilpatrick, W. Li, B. P. Padley, R. Redjimi, J. Roberts, J. Rorie, W. Shi, Z. Tu, J. Zabel, A. Zhang

University of Rochester, Rochester, USA

A. Bodek, P. de Barbaro, R. Demina, Y. t. Duh, J. L. Dulemba, C. Fallon, T. Ferbel, M. Galanti, A. Garcia-Bellido, J. Han, O. Hindrichs, A. Khukhunaishvili, P. Tan, R. Taus

Rutgers, The State University of New Jersey, Piscataway, USA

A. Agapitos, J. P. Chou, Y. Gershtein, E. Halkiadakis, M. Heindl, E. Hughes, S. Kaplan, R. Kunnawalkam Elayavalli, S. Kyriacou, A. Lath, R. Montalvo, K. Nash, M. Osherson, H. Saka, S. Salur, S. Schnetzer, D. Sheffield, S. Somalwar, R. Stone, S. Thomas, P. Thomassen, M. Walker

University of Tennessee, Knoxville, USA

A. G. Delannoy, J. Heideman, G. Riley, S. Spanier

Texas A & M University, College Station, USA

O. Bouhali[72], A. Celik, M. Dalchenko, M. De Mattia, A. Delgado, S. Dildick, R. Eusebi, J. Gilmore, T. Huang, T. Kamon[73], S. Luo, R. Mueller, D. Overton, L. Perniè, D. Rathjens, A. Safonov

Texas Tech University, Lubbock, USA

N. Akchurin, J. Damgov, F. De Guio, P. R. Dudero, S. Kunori, K. Lamichhane, S. W. Lee, T. Mengke, S. Muthumuni, T. Peltola, S. Undleeb, I. Volobouev, Z. Wang

Vanderbilt University, Nashville, USA

S. Greene, A. Gurrola, R. Janjam, W. Johns, C. Maguire, A. Melo, H. Ni, K. Padeken, J. D. Ruiz Alvarez, P. Sheldon, S. Tuo, J. Velkovska, M. Verweij, Q. Xu

University of Virginia, Charlottesville, USA

M. W. Arenton, P. Barria, B. Cox, R. Hirosky, M. Joyce, A. Ledovskoy, H. Li, C. Neu, T. Sinthuprasith, Y. Wang, E. Wolfe, F. Xia

Wayne State University, Detroit, USA

R. Harr, P. E. Karchin, N. Poudyal, J. Sturdy, P. Thapa, S. Zaleski

University of Wisconsin - Madison, Madison, WI, USA

M. Brodski, J. Buchanan, C. Caillol, D. Carlsmith, S. Dasu, L. Dodd, B. Gomber, M. Grothe, M. Herndon, A. Hervé, U. Hussain, P. Klabbers, A. Lanaro, K. Long, R. Loveless, T. Ruggles, A. Savin, V. Sharma, N. Smith, W. H. Smith, N. Woods

[†] **Deceased**

1: Also at Vienna University of Technology, Vienna, Austria
2: Also at IRFU, CEA, Université Paris-Saclay, Gif-sur-Yvette, France
3: Also at Universidade Estadual de Campinas, Campinas, Brazil
4: Also at Federal University of Rio Grande do Sul, Porto Alegre, Brazil
5: Also at Université Libre de Bruxelles, Bruxelles, Belgium
6: Also at University of Chinese Academy of Sciences, Beijing, China
7: Also at Institute for Theoretical and Experimental Physics, Moscow, Russia
8: Also at Joint Institute for Nuclear Research, Dubna, Russia

9: Also at Fayoum University, El-Fayoum, Egypt

10: Now at British University in Egypt, Cairo, Egypt

11: Now at Helwan University, Cairo, Egypt

12: Also at Department of Physics, King Abdulaziz University, Jeddah, Saudi Arabia

13: Also at Université de Haute Alsace, Mulhouse, France

14: Also at Skobeltsyn Institute of Nuclear Physics, Lomonosov Moscow State University, Moscow, Russia

15: Also at CERN, European Organization for Nuclear Research, Geneva, Switzerland

16: Also at RWTH Aachen University, III. Physikalisches Institut A, Aachen, Germany

17: Also at University of Hamburg, Hamburg, Germany

18: Also at Brandenburg University of Technology, Cottbus, Germany

19: Also at MTA-ELTE Lendület CMS Particle and Nuclear Physics Group, Eötvös Loránd University, Budapest, Hungary

20: Also at Institute of Nuclear Research ATOMKI, Debrecen, Hungary

21: Also at Institute of Physics, University of Debrecen, Debrecen, Hungary

22: Also at Indian Institute of Technology Bhubaneswar, Bhubaneswar, India

23: Also at Institute of Physics, Bhubaneswar, India

24: Also at Shoolini University, Solan, India

25: Also at University of Visva-Bharati, Santiniketan, India

26: Also at Isfahan University of Technology, Isfahan, Iran

27: Also at Plasma Physics Research Center, Science and Research Branch, Islamic Azad University, Tehran, Iran

28: Also at Università degli Studi di Siena, Siena, Italy

29: Also at Scuola Normale e Sezione dell'INFN, Pisa, Italy

30: Also at Kyunghee University, Seoul, Korea

31: Also at International Islamic University of Malaysia, Kuala Lumpur, Malaysia

32: Also at Malaysian Nuclear Agency, MOSTI, Kajang, Malaysia

33: Also at Consejo Nacional de Ciencia y Tecnología, Mexico city, Mexico

34: Also at Warsaw University of Technology, Institute of Electronic Systems, Warsaw, Poland

35: Also at Institute for Nuclear Research, Moscow, Russia

36: Now at National Research Nuclear University 'Moscow Engineering Physics Institute' (MEPhI), Moscow, Russia

37: Also at St. Petersburg State Polytechnical University, St. Petersburg, Russia

38: Also at University of Florida, Gainesville, USA

39: Also at P.N. Lebedev Physical Institute, Moscow, Russia

40: Also at California Institute of Technology, Pasadena, USA

41: Also at Budker Institute of Nuclear Physics, Novosibirsk, Russia

42: Also at Faculty of Physics, University of Belgrade, Belgrade, Serbia

43: Also at INFN Sezione di Pavia [a], Università di Pavia [b], Pavia, Italy

44: Also at University of Belgrade, Faculty of Physics and Vinca Institute of Nuclear Sciences, Belgrade, Serbia

45: Also at National and Kapodistrian University of Athens, Athens, Greece

46: Also at Riga Technical University, Riga, Latvia

47: Also at Universität Zürich, Zurich, Switzerland

48: Also at Stefan Meyer Institute for Subatomic Physics (SMI), Vienna, Austria

49: Also at Gaziosmanpasa University, Tokat, Turkey

50: Also at Adiyaman University, Adiyaman, Turkey

51: Also at Istanbul Aydin University, Istanbul, Turkey

52: Also at Mersin University, Mersin, Turkey

53: Also at Piri Reis University, Istanbul, Turkey

54: Also at Ozyegin University, Istanbul, Turkey

55: Also at Izmir Institute of Technology, Izmir, Turkey

56: Also at Marmara University, Istanbul, Turkey

57: Also at Kafkas University, Kars, Turkey

58: Also at Istanbul University, Faculty of Science, Istanbul, Turkey

59: Also at Istanbul Bilgi University, Istanbul, Turkey

60: Also at Hacettepe University, Ankara, Turkey

61: Also at Rutherford Appleton Laboratory, Didcot, United Kingdom

62: Also at School of Physics and Astronomy, University of Southampton, Southampton, United Kingdom

63: Also at Monash University, Faculty of Science, Clayton, Australia

64: Also at Bethel University, St. Paul, USA

65: Also at Karamanoğlu Mehmetbey University, Karaman, Turkey

66: Also at Utah Valley University, Orem, USA

67: Also at Purdue University, West Lafayette, USA

68: Also at Beykent University, Istanbul, Turkey

69: Also at Bingol University, Bingol, Turkey

70: Also at Sinop University, Sinop, Turkey

71: Also at Mimar Sinan University, Istanbul, Istanbul, Turkey

72: Also at Texas A&M University at Qatar, Doha, Qatar

73: Also at Kyungpook National University, Daegu, Korea